Supplementary Information File

1. Methodology

1.1. *In Silico* Investigations

1.1.1. SwissADME

The SwissADME online tool was used to determine the pharmacokinetic properties of the synthesized compounds. It is a platform offering a thorough evaluation of absorption, distribution, metabolism and excretion (ADME) parameters in accordance with the molecular structure of compounds. Molecular drawing software was first used to draw the chemical structures of the chalcone sulfonate esters synthesized and convert the structure into canonical SMILES format. This was followed by submission to the SwissADME server to be evaluated computationally using these SMILES. SwissADME computes a number of physicochemical and pharmacokinetic descriptors of a substance such as molecular weight, lipophilicity (LogP), hydrogen bond donors and acceptors, topological polar surface area (TPSA), gastrointestinal (GI) absorption, blood-brain barrier (BBB) permeability, water solubility, and drug-likeness based on a given set of rules that include Lipinski, Ghose, Veber, Egan, and Muegge filters. Passive gastrointestinal absorption and brain penetration were also predicted with the use of the BOILED-Egg model that is present in SwissADME. The comparison of ADME profiles of the synthesized compounds with two reference drugs, Thiourea and Acarbose were used to determine their pharmacokinetic suitability [1].

1.1.2. Molecular docking

1.1.2.1. Protein Selection and Protein Preparation

In the case of molecular docking analysis, two enzymes related to metabolic and pathogenic activities were chosen: urease and α-amylase. Urease is a major virulence factor that is involved in the hydrolysis of urea and is highly implicated in gastric and urinary tract infections, whereas

α-amylase is a major enzyme in carbohydrate metabolism and is also a highly targeted enzyme in the management of diabetes mellitus. These proteins had their three-dimensional crystal structures obtained at the Protein Data Bank (PDB). In the case of urease, 1OTH and 2ZAV were selected as the protein structures, and 1SMD and 5U3A were selected in the case of alpha amylase. The proteins of choice had high resolution and clearly defined active sites, which could be used in docking experiments. Table 1 contains the information about the chosen proteins, their PDB code, resolution, and their natural source in detail. Protein structures were made ready through Molegro Virtual Docker (MVD) before docking. The protein structures were washed with all co-crystallized ligands, water molecules and other non-essential heteroatoms to avoid interference with the ligand binding. Stabilization of the protein structure by polar hydrogen atoms was done, and the bond orders were given. The minimization of energy of the protein structures was done in order to eliminate steric clashes and ensure the geometry of the active site residues is optimized. The ready proteins were then stored in the right format for docking simulations [2].

2.3.2.2. Ligand Preparation

The ligands (synthesized chalcone sulfonate esters, compounds **1-7**) and template drugs (thiourea urease inhibitor) and acarbose (α-amylase inhibitor) were applied to the docking study. The molecular modeling software and three-dimensional conformations of the synthesized compounds were obtained by drawing the chemical structures of the compounds. Optimization of the geometries of the ligands was done to produce conformers that were stable before docking. Hydrogen atoms were incorporated in order to make the valence and molecular geometry right. Every ligand was then minimized in terms of energy to get the lowest energy conformations to be used in docking simulations. The ligands were prepared and then exported to Molegro Virtual Docker to be analyzed by docking [3].

2.3.2.3. Molecular Docking Assay

The simulations of the molecular docking were conducted with Molegro Virtual Docker (MVD) to determine the binding interactions between the synthesized chalcone sulfonate ester derivatives and the chosen target proteins. The docking protocol was created to come up with the optimal binding orientations of the ligands in the active sites of the enzymes. To begin with, the ready protein structures were loaded into the Molegro Virtual Docker workspace. The binding sites of each protein were determined using the cavity detection algorithm applied to the MVD, which identifies potential ligand-binding pockets based on the protein surface topology. Docking was performed in the cavity with the highest volume and the most relevance to the catalytic site [4]. Prediction of the ligand conformation within the binding site was performed using the MolDock optimizer, which employs a guided differential evolution algorithm during the docking process. The MolDock scoring feature was used to approximate the binding affinity of each ligand for the target proteins. The ligands were free to undergo conformational changes to take up different orientations and positions in the active site cavity in the docking process. The ligands were docked repeatedly to have consistent and reliable results. The poses generated by docking were ranked by MolDock score, and lower energy values corresponded to good binding interactions. Based on the lowest binding energy and the highest affinity of the key amino acids that were observed in the active site, the optimal docking geometry of each ligand-protein complex was selected [5].

Table S1: Selection of Urease and α-Amylase protein structures used for molecular docking

S. No.	Enzyme System	Selected Protein Target	PDB ID	Resolution (Å)	Reference
1	Urea Metabolism (Human Urea Cycle)	Ornithine Transcarbamylase	**1OTH**	2.05	[6]
2	Urea Metabolism (Human Urea Cycle)	Arginase I	**2ZAV**	1.55	[7]
3	Carbohydrate Metabolism	Salivary α-Amylase	**1SMD**	1.80	[8]
4	Carbohydrate Metabolism	Pancreatic α-Amylase	**5U3A**	1.65	[9]

2.3.2.4. Visualization

Three-dimensional structures showed scientists the spatial orientation of ligands in the active binding site, while two-dimensional interaction diagrams displayed the specific hydrogen bonds, hydrophobic interactions, π-π interactions, and van der Waals contacts which ligands established with amino acid residues of the target proteins [10].

2.3.2.5. Validation of Docking

To confirm the correctness and reliability of the molecular docking protocol employed in the present paper, a redocking experiment was conducted. Redocking is the conventional validation technique whereby the co-crystallized ligand within the protein crystal structure is removed and re-docked into the same binding cavity. The resultant predicted docking pose is compared to the experimentally obtained ligand conformation of the crystal structure. Root Mean Square Deviation (RMSD) is used to measure the similarity of these two poses. In the current research, redocking validation of the identified target proteins to be utilized in the docking experiment [the urease proteins 1OTH and 2ZAV, the alpha-amylase proteins 1SMD and 5U3A] was performed, and the redocking results were obtained in the Protein Data Bank

(PDB). The native ligands of the proteins were then re-docked into their active sites under the same docking parameters used for the synthesized chalcone sulfonate esters. To measure the accuracy of the docking protocol, the Root Mean Square Deviation (RMSD) between the redocked and crystallographic ligand poses was determined. RMSD is used to evaluate the mean distance between atoms of the two conformations. An RMSD value of less than 2.0 Å is usually accepted in molecular docking validation studies and indicates that the docking protocol reproduces the experimental binding mode correctly [11].

2.4. MD Simulation

To further analyze the stability and dynamic behavior of the most promising protein-ligand complexes identified as a result of docking studies of chalcone sulfonate esters, the MD simulations were conducted on the WebGRO platform. WebGRO is an online interface to the popular molecular simulation program GROMACS, through which it is possible to efficiently simulate biomolecular systems using MD. The protein-ligand complexes that were used in the MD simulations included Compound **7** with 2ZAV and compound **5** with 5U3A, since the complexes had good docking interactions and binding affinities. The uploaded complexes were docked into the WebGRO server to simulate them. In the process of system preparation, the GROMOS96 43a1 force field was used to model the molecular interactions of the protein with the topology of the ligand being created automatically by the server. The solvation of the ligands was carried out in a cubic simulation box saturated with SPC water molecules, with a distance of at least 1.0 nm between the protein surface and the box boundary to ensure sufficient solvation. In order to ensure neutrality of the system, it was neutralized with corresponding counter ions (Na^+ or Cl^-) [12].

The steepest descent algorithm was used to minimize energy to remove steric clashes and bad contacts in the system. The system was equilibrated under two ensembles after the system had been minimized in terms of energy. To stabilize the temperature of the system at 300 K, NVT

(volume, temperature, fixed number of particles) equilibration was done. This was then followed by equilibration of NPT (number of particles, pressure, and temperature constant), to stabilize pressure at 1 bar to enable the system density to equilibrate adequately. A 25 ns production MD simulation of each of the protein -ligand complexes was conducted after successful equilibration. During the simulation, periodicity was used in three dimensions. The simulation results were then studied to assess stability in structure and behavior of interactions based on some parameters, including root mean square deviation (RMSD), root mean square fluctuation (RMSF), radius of gyration (Rg), hydrogen bond formation, and the solvent accessible surface area (SASA). These parameters will give information on the conformational stability, flexibility, compactness, persistence of interactions and the solvent exposure of the protein-ligand complexes [13].

2.5. Density functional theory (DFT)

All quantum chemical calculations were performed using the Gaussian 09 computational chemistry package. Initially, the molecular structures of the selected lead compounds were constructed and prepared in their molecular form. Geometry optimization was carried out using the DFT method with the 6-311G basis set and the B3LYP functional. This level of theory is widely applied for investigating the electronic properties and structural stability of organic molecules because it provides a suitable balance between computational efficiency and accuracy [14]. The optimization process for geometry allowed molecules to reach their most stable states because no symmetry constraints were used during the process. The absence of imaginary frequencies in the vibrational analysis proved that the optimized structures remained stable. The optimization process produced calculations for multiple electronic parameters, which included the highest occupied molecular orbital (HOMO) and lowest unoccupied molecular orbital (LUMO) energy values, along with energy gap (ΔE) and global reactivity descriptors and molecular electrostatic potential (MEP) of the system [15]. The frontier molecular

orbital (FMO) analysis assessed how the molecules donated and accepted electrons. The study derived global reactivity descriptors, which included ionization potential (I), electron affinity (A), chemical hardness (η), chemical softness (S), chemical potential (μ) and electrophilicity index (ω) from the HOMO and LUMO energies based on Koopmans' theorem. The generation of molecular electrostatic potential maps enabled the detection of electrophilic and nucleophilic reactive areas present in the molecules.

Multiwfn software tools were used to study electron sharing between atoms and their non-bonding interactions [16]. The wavefunction data obtained from the DFT calculations were converted into formatted checkpoint (.fchk) files and used as input for wavefunction analysis. Electron localization characteristics were investigated through Electron Localization Function (ELF) and Localized Orbital Locator (LOL) analyses, while weak intermolecular interactions were examined using Reduced Density Gradient (RDG) and Non-Covalent Interaction (NCI) analyses. RDG scatter plots and NCI surfaces were generated to identify attractive interactions, van der Waals forces, and steric repulsion within the studied compounds [17].

References

1. M. Guerfi, M. Berredjem, A. Dekir, R. Bahadi, S.-E. Djouad, T. O. Sothea, R. Redjemia, B. Belhani and M. Boussaker, *Molecular Diversity*, 2024, **28**, 1023-1038.
2. M. A. Mp, C. P. Somaiya, P. K. Singhal, A. K. Nigam, A. Mukherjee and K. P. Baalann10, *Tuijin Jishu/Journal of Propulsion Technology*, 2023, **44**, 2023.
3. D. S. Megawati, J. Ekowati and S. Siswodihardjo, *Letters in Drug Design & Discovery*, 2024, **21**, 3913-3922.
4. J. Monga, N. S. Ghosh, S. Kamboj and M. Mukhija, *Journal of Molecular Chemistry*, 2023, **3**, 590-590.
5. R. Gupta, A. Raza, S. K. Singh, J. Kaur and P. Wadhwa, *Current Signal Transduction Therapy*, 2025, **20**, E15743624305290.

6. D. Shi, H. Morizono, Y. Ha, M. Aoyagi, M. Tuchman and N. M. Allewell, *Journal of Biological Chemistry*, 1998, **273**, 34247-34254.

7. L. Di Costanzo, M. E. Pique and D. W. Christianson, *Journal of the American Chemical Society*, 2007, **129**, 6388-6389.

8. N. Ramasubbu, V. Paloth, Y. Luo, G. D. Brayer and M. J. Levine, *Biological Crystallography*, 1996, **52**, 435-446.

9. L. Goldbach, B. J. Vermeulen, S. Caner, M. Liu, C. Tysoe, L. van Gijzel, R. Yoshisada, M. Trellet, H. van Ingen and G. D. Brayer, *ACS chemical biology*, 2019, **14**, 1751-1759.

10. A. T. Agustin, A. I. Muflihah, A. F. Wijaya, H. Mufidah and J. Riranto.

11. A. D. Savitri, H. B. Hidayati, L. Veterini, M. S. Widyaswari, A. R. Muhammad, A. Fairus, M. Q. B. Zulfikar, M. Astri, N. A. Ramasima and D. P. Anggraeni, *JJBS: Jordan Journal of Biological Sciences*, 2023, **16**, 7-12.

12. S. Karakkadparambil Sankaran and A. S. Nair, *Journal of Biomolecular Structure and Dynamics*, 2023, **41**, 6459-6475.

13. M. Hussain, N. Kanwal, A. Jahangir, N. Ali, N. Hanif and O. Ullah, *Frontiers in Chemistry*, 2024, **12**, 1493165.

14. K. Gören, E. Çimen, V. Tahiroğlu and Ü. Yıldıko, *Bitlis Eren Üniversitesi Fen Bilimleri Dergisi*, 2024, **13**, 659-672.

15. N. Karakuş, *Cumhuriyet Science Journal*, 2024, **45**, 282-290.

16. K. Arulaabaranam, S. Muthu, G. Mani and A. B. Geoffrey, *Heliyon*, 2021, **7**.

17. F. Akman, A. Demirpolat, A. S. Kazachenko, A. S. Kazachenko, N. Issaoui and O. Al-Dossary, *Molecules*, 2023, **28**, 2684.

2. Results and Discussion

2.1. ADME Studies

Table S2: SwissADME-predicted properties of synthesized compounds **(1-7)**

Compounds	**1**	**2**	**3**	**4**	**5**	**6**	**7**
Physicochemical properties							
MW	406.49	443.31	394.44	398.86	414.47	398.86	409.41
#Heavy atoms	29	27	28	27	30	27	29
#Aromatic heavy atoms	18	18	18	18	22	18	18
Fraction Csp3	0.12	0	0.05	0	0	0	0
#Rotatable bonds	6	6	7	6	6	6	7
#H-bond acceptors	4	4	5	4	4	4	6
#H-bond donors	0	0	0	0	0	0	0
MR	115.45	108.25	107.04	105.56	118.05	105.56	109.37
TPSA	68.82	68.82	78.05	68.82	68.82	68.82	114.64
Lipophilicity							
iLOGP	3.79	3.57	3.23	3.46	3.22	2.79	2.71
XLOGP3	5.88	5.48	4.76	5.42	6.04	5.42	4.62
WLOGP	6.25	6.08	5.33	5.98	6.48	5.98	5.23
MLOGP	4.64	4.59	3.65	4.48	4.67	4.48	3.03
Silicos-IT Log P	5.5	4.59	3.98	4.56	4.96	4.56	1.76
Consensus Log P	5.21	4.86	4.19	4.78	5.07	4.64	3.47
Water solubility							
ESOL Log S	-6.13	-6.14	-5.3	-5.82	-6.36	-5.82	-5.29
ESOL Class	Poorly	Poorly	Moderatel	Moderatel	Poorly	Moderatel	Moder

	soluble	soluble	y soluble	y soluble	soluble	y soluble	ately soluble
Pharmacokinetics							
GI absorption	High	High	High	High	High	High	Low
BBB permeant	No	No	No	No	No	No	No
Pgp substrate	Yes	Yes	No	Yes	Yes	Yes	Yes
CYP1A2 inhibitor	Yes	Yes	No	Yes	No	Yes	Yes
CYP2C19 inhibitor	Yes	Yes	Yes	Yes	Yes	Yes	Yes
CYP2C9 inhibitor	Yes	Yes	Yes	Yes	No	Yes	Yes
CYP2D6 inhibitor	No	No	No	No	No	No	No
CYP3A4 inhibitor	No	No	No	No	No	No	No
log Kp (cm/s)	-4.6	-5.11	-5.33	-4.88	-4.54	-4.88	-5.52
Drug-likeness							
Lipinski #violations	1	1	0	1	1	1	0
Ghose #violations	1	1	0	1	1	1	0
Veber #violations	0	0	0	0	0	0	0
Egan #violations	1	1	0	1	1	1	0
Muegge #violations	1	1	0	1	1	1	0
Bioavailability Score	0.55	0.55	0.55	0.55	0.55	0.55	0.55
Medicinal chemistry							
PAINS #alerts	0	0	0	0	0	0	0
Brenk #alerts	2	2	2	2	2	2	4
Leadlikeness #violations	2	2	2	2	2	2	2
Synthetic Accessibility	3.84	3.46	3.52	3.44	3.67	3.45	3.52

2.2. Molecular Docking Studies

Table S3: Represented molecular docking interactions of Thiourea (reference drug) and synthesized compounds **(1-7)** against urease proteins (1OTH and 2ZAV)

Compound	PDB ID	Docking score	H-Bonds	Protein-ligand interaction by H-bonding				Protein-ligand interaction by hydrophobic interaction			
				Amino acid residue	Distance (Å)	Category	Type	Amino acid residue	Distance (Å)	Category	Type
1	**1OTH**	-130.668	-1.19515	ARG 270	2.39048	H-Bond	Conventional H-Bond	ASP165:C,O; LEU166:N	3.56002	Hydrophobic	Amide-Pi Stacked
				ASN 198	2.43418	H-Bond	C-H Bond				
				HIS 202	2.16974	H-Bond	C-H Bond	LEU 166	3.88068	Hydrophobic	Alkyl
				SER 267	2.46563	H-Bond	C-H Bond	HIS 202	4.34338	Hydrophobic	Pi-Alkyl
								ARG 270	5.4336	Hydrophobic	Pi-Alkyl
								LEU 166	4.85452	Hydrophobic	Pi-Alkyl
2		-128.498	-1.20046	ARG 270	2.36671	H-Bond	Conventional H-Bond	ASP165:C,O; LEU166:N	3.52563	Hydrophobic	Amide-Pi Stacked
				ASN 198	2.32601	H-Bond	C-H Bond				
				HIS 202	2.23048	H-Bond	C-H Bond	ARG 270	5.48288	Hydrophobic	Pi-Alkyl
				SER 267	2.35247	H-Bond	C-H Bond	LEU 166	4.79882	Hydrophobic	Pi-Alkyl
3		-129.672	-2.83477	ARG 270	1.787	H-Bond	Conventional H-Bond	TYR 223	4.63895	Hydrophobic	Pi-Pi T-shaped
				ARG 277	2.43784	H-Bond	Conventional H Bond	LEU 163	4.69643	Hydrophobic	Alkyl
				ASN 198	2.73475	H-Bond	C-H Bond	MET 268	4.83924	Hydrophobic	Alkyl
				TYR 223	2.65692	H-Bond	C-H Bond				
				MET 268	2.75964	H-Bond	C-H Bond				
4		-122.404	-1.51843	ARG 270	1.81977	H-Bond	Conventional H-Bond	TYR 223	4.61099	Hydrophobic	Pi-Pi T-shaped
				ARG 277	2.18071	H-Bond	Conventional H Bond	LEU 163	5.05453	Hydrophobic	
				ASN 198	2.83424	H-Bond	C-H Bond	ARG 270	5.36322	Hydrophobic	Alkyl

				TYR 223	2.51544	H-Bond	C-H Bond				Pi-Alkyl
5			-5.31263	SER 267	2.3099	H-Bond	Conventional H-Bond	LEU 163	2.2983	Hydrophobic	Pi-Sigma
				MET 268	1.9339	H-Bond	Conventional H Bond	MET 268	4.64814	Hydrophobic	Pi-Alkyl
		-132.168		SER 267	2.56005	H-Bond	C-H Bond	LEU 163	4.96282	Hydrophobic	Pi-Alkyl
				SER 267	2.74008	H-Bond	C-H Bond	CYS 303	4.34474	Hydrophobic	Pi-Alkyl
								CYS 303	4.74069	Hydrophobic	Pi-Alkyl
6			0	ARG 270	2.78414	H-Bond	Conventional H-Bond				
		-121.812		LEU 166	2.6879	H-Bond	C-H Bond				
				HIS 202	2.61808	H-Bond	C-H Bond				
				TYR 223	3.04346	H-Bond	C-H Bond				
7				SER 267	2.41764	H-Bond	Conventional H-Bond	ASN 198	2.63752	Hydrophobic	Pi-Sigma
				ARG 270	2.48966	H-Bond	Conventional H-Bond	TYR 223	5.60402	Hydrophobic	Pi-Pi T-shaped
				ARG 270	2.23418	H-Bond	Conventional H-Bond				
		-137.29	-2.8346	ARG 270	2.78864	H-Bond	Conventional H-Bond				
				ARG 277	2.65671	H-Bond	Conventional H-Bond				
				ARG 277	1.64243	H-Bond	Conventional H-Bond				
				SER 267	2.317	H-Bond	C-H Bond				
				ARG 270	1.85238	H-Bond	C-H Bond				
Thiourea			-4.25292	GLY 197	2.27823	H-Bond	Conventional H-Bond				
		-67.354		GLY 197	1.89746	H-Bond	Conventional H-Bond				
				GLU 224	2.07603	H-Bond	Conventional H-Bond				
1	**2ZAV**		-3.21246	LYS 68	2.50851	H-Bond	Conventional H-Bond	ILE 166	2.88632	Hydrophobic	Pi-Sigma
				LYS 68	2.67146	H-Bond	Conventional H-Bond	ILE 166	4.11953	Hydrophobic	Alkyl
				TYR 218	2.91728	H-Bond	Conventional H-Bond	PRO 63	4.06094	Hydrophobic	Alkyl
		-147.842		ARG 222	1.6318	H-Bond	Conventional H-Bond	PRO 20	5.07391	Hydrophobic	Pi-Alkyl
				GLY 221	2.73233	H-Bond	C-H Bond	LYS 172	4.32373	Hydrophobic	Pi-Alkyl
				ASN 139	3.08877	H-Bond	Pi-Donor C-H Bond	ARG 222	4.19718	Hydrophobic	Pi-Alkyl

2		-2.5	ASN 69	1.92623	H-Bond	Conventional H-Bond	LEU 206	2.8133	Hydrophobic	Pi-Sigma
			LYS 68	2.79789	H-Bond	C-H Bond	PHE 198	5.74606	Hydrophobic	Pi-Pi
			LYS 196	2.25558	H-Bond	C-H Bond	LYS 17	4.47372	Hydrophobic	Stacked
	-140.214		LYS 196	2.59289	H-Bond	C-H Bond	PRO 63	5.43504	Hydrophobic	Alkyl
							LYS 68	3.86481	Hydrophobic	Pi-Alkyl
							LYS 196	5.10692	Hydrophobic	Pi-Alkyl
										Pi-Alkyl
3		-4.76894	LYS 17	1.75441	H-Bond	Conventional H-Bond	GLN19:C,O;P	3.38145	Hydrophobic	Amide-Pi
			LYS 68	2.41673	H-Bond	Conventional H-Bond	RO20:N			Stacked
			TYR 218	2.27153	H-Bond	Conventional H-Bond	PRO 63	4.13909	Hydrophobic	Alkyl
	-149.239		LYS 17	2.61347	H-Bond	C-H-Bond	PRO 20	4.10608	Hydrophobic	Pi-Alkyl
			LYS 196	2.75947	H-Bond	C-H Bond	LYS 68	4.19662	Hydrophobic	Pi-Alkyl
			GLU 214	3.08627	H-Bond	C-H Bond	LYS 68	3.97169	Hydrophobic	Pi-Alkyl
							LYS 196	5.00458	Hydrophobic	Pi-Alkyl
4		-3.79141	LYS 68	1.91549	H-Bond	Conventional H-Bond	ARG 222	4.30123	Hydrophobic	Pi-Alkyl
	-138.582		LYS 223	2.07928	H-Bond	Conventional H-Bond	ILE 66	5.27691	Hydrophobic	Pi-Alkyl
							LYS 172	3.71678	Hydrophobic	Pi-Alkyl
5		-2.5	ASN 69	1.99771	H-Bond	Conventional H-Bond	LEU 206	2.81541	Hydrophobic	Pi-Sigma
			LYS 68	2.77049	H-Bond	C-H-Bond	PHE 198	5.70229	Hydrophobic	Pi-Pi
			LYS 196	2.21364	H-Bond	C-H Bond	LYS 68	3.92701	Hydrophobic	Stacked
	-154.429						LYS 196	5.03071	Hydrophobic	Pi-Alkyl
							LYS 17	5.08049	Hydrophobic	Pi-Alkyl
										Pi-Alkyl
6		-6.61711	LYS 17	2.08411	H-Bond	Conventional H-Bond	TYR 197	5.23934	Hydrophobic	Pi-Pi T-
			ASN 69	1.62835	H-Bond	Conventional H-Bond	LYS 191	5.12792	Hydrophobic	shaped
	-129.174		TYR 197	1.804	H-Bond	Conventional H-Bond	PRO 20	4.88202	Hydrophobic	Pi-Alkyl
			LYS 196	2.77417	H-Bond	C-H Bond	LYS 196	4.92511	Hydrophobic	Pi-Alkyl
										Pi-Alkyl

7	-171.22	-8.6456	LYS 17	2.69002	H-Bond	Conventional H-Bond	PRO 63	5.31858	Hydrophobic	Pi-Alkyl
			LYS 17	2.15443	H-Bond	Conventional H-Bond	PRO 20	4.85571	Hydrophobic	Pi-Alkyl
			LYS 17	2.33558	H-Bond	Conventional H-Bond	LYS 68	4.73572	Hydrophobic	Pi-Alkyl
			ASN 69	2.43176	H-Bond	Conventional H-Bond	LYS 196	5.14516	Hydrophobic	Pi-Alkyl
			ASN 69	1.81164	H-Bond	Conventional H-Bond	LYS 196	4.85213	Hydrophobic	Pi-Alkyl
			LYS 191	2.42223	H-Bond	Conventional H-Bond				
			LYS 68	2.72046	H-Bond	Conventional H-Bond				
			GLY 194	2.64408	H-Bond	C-H Bond				
Thiourea	-70.611	-6.4032	ILE 58	2.83724	H-Bond	Conventional H-Bond				
			SER 72	3.08641	H-Bond	Conventional H-Bond				
			PHE 55	2.03755	H-Bond	Conventional H-Bond				
			ASP 57	1.87507	H-Bond	Conventional H-Bond				
			PHE 55	2.27528	H-Bond	Conventional H-Bond				

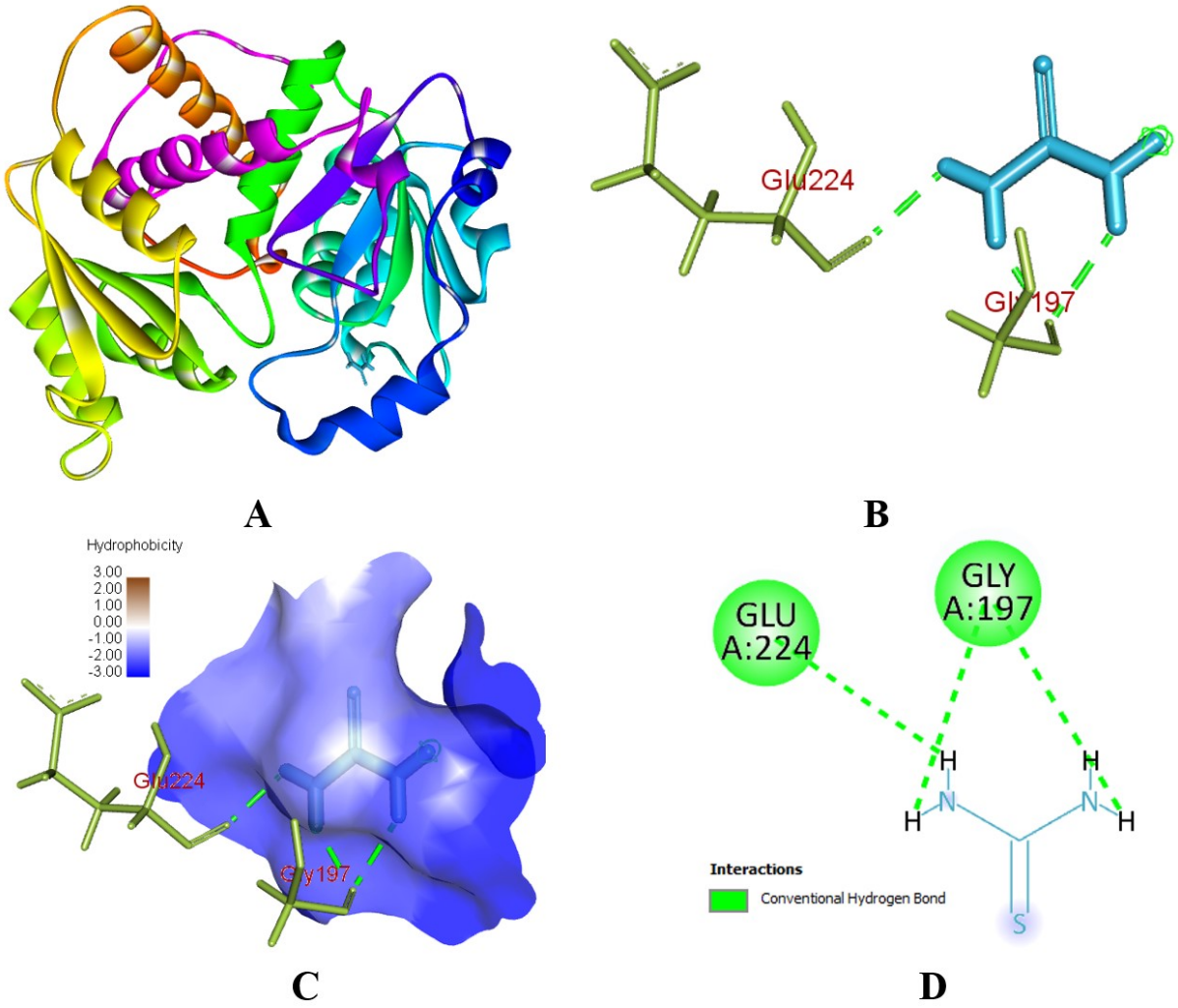

Figure S1: Interaction of 1OTH protein with Thiourea (A) structure of protein (B) protein-ligand interaction (C) hydrophobic interaction (D) 2D diagram of ligand

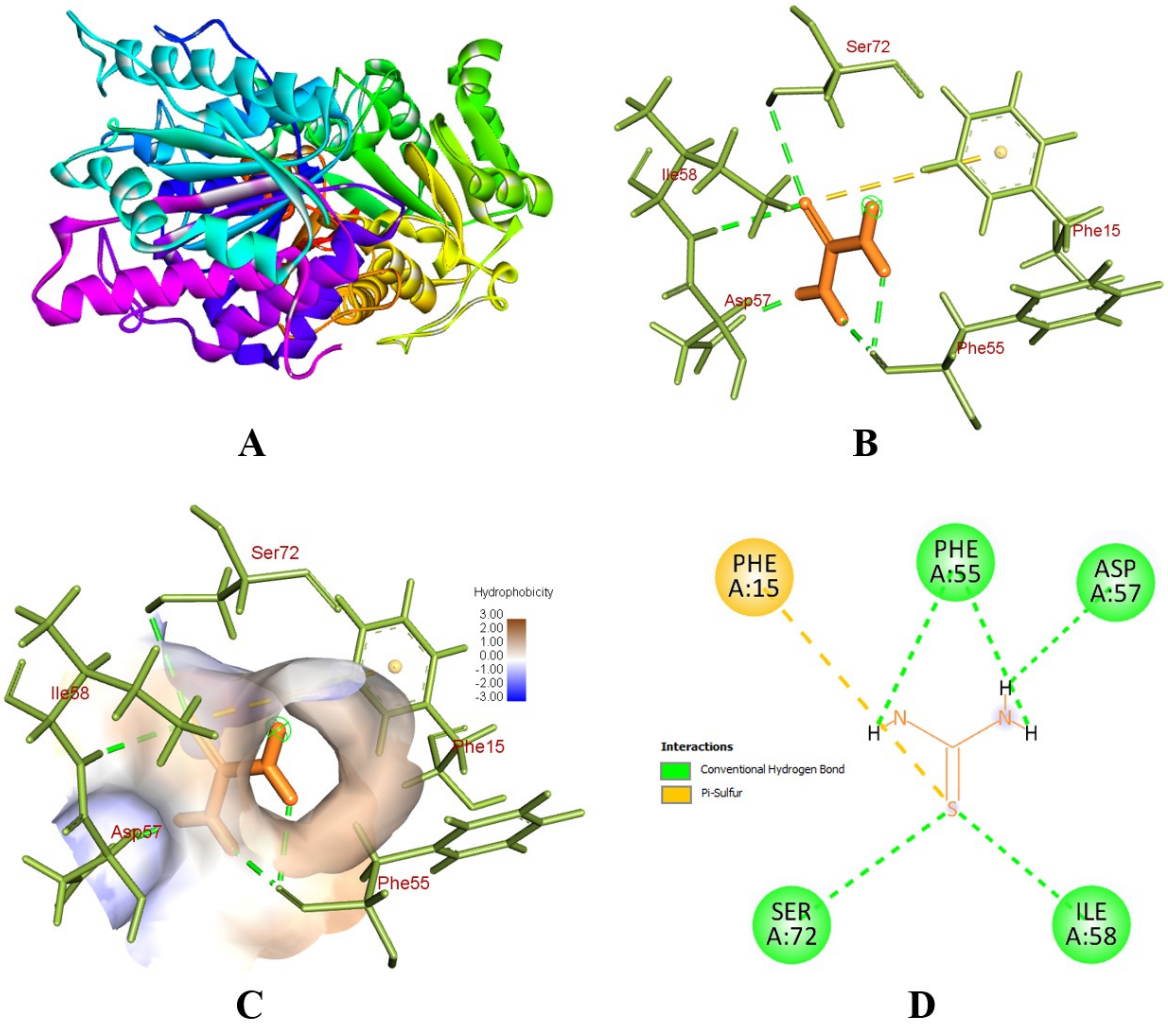

Figure S2: Interaction of 2ZVA protein with Thiourea (A) structure of protein (B) protein-ligand interaction (C) hydrophobic interaction (D) 2D diagram of ligand

Table S4: Represented molecular docking interactions of Acarbose (reference drug) and synthesized compounds **(1-7)** against α-amylase proteins (ISMD and 5U3A)

Compound	PDB ID	Docking score	H-Bonds	Protein-ligand interaction by H-bonding				Protein-ligand interaction by hydrophobic interaction			
				Amino acid residue	Distance (Å)	Category	Type	Amino acid residue	Distance (Å)	Category	Type
1	**1SMD**	-122.523	0	HIS 201	2.57477	H-Bond	C-H Bond	TYR 62	4.06583	Hydrophobic	Pi-Pi Stacked
								HIS 201	4.39658	Hydrophobic	Pi-Pi T-shaped
								TRP 58	5.08119	Hydrophobic	Pi-Alkyl
								TRP 58	4.30347	Hydrophobic	Pi-Alkyl
								TRP 59	3.98805	Hydrophobic	Pi-Alkyl
								HIS 305	4.35167	Hydrophobic	Pi-Alkyl
								ALA 198	4.9098	Hydrophobic	Pi-Alkyl
								LYS 200	4.47151	Hydrophobic	Pi-Alkyl
								ILE 235	4.58687	Hydrophobic	Pi-Alkyl
2		-116.956	0	SER 163	2.80705	H-Bond	C-H Bond	HIS 305	4.62483	Hydrophobic	Pi-Pi T-shaped
				HIS 305	2.37184	H-Bond	C-H Bond	LEU 162	4.65841	Hydrophobic	Alkyl
								LEU 165	5.22929	Hydrophobic	Pi-Alkyl
								LEU 162	4.47	Hydrophobic	Pi-Alkyl
3		-116.33	-1.55432	GLN 63	2.25767	H-Bond	Conventional H-Bond	TYR 62	4.12342	Hydrophobic	Pi-Pi Stacked
				ASP 300	2.62308	H-Bond		LEU 165	4.90831	Hydrophobic	Pi-Alkyl
				ASP 300	2.64886	H-Bond	C-H Bond				
							C-H Bond				
4		-121.181	0	HIS 201	2.46823	H-Bond	C-H Bond	TYR 62	4.09448	Hydrophobic	Pi-Pi T-shaped
								HIS 201	4.48029	Hydrophobic	Pi-Pi T-shaped
								ALA 198	5.12293	Hydrophobic	Pi-Alkyl
								LYS 200	4.35369	Hydrophobic	Pi-Alkyl
								ILE 135	4.39439	Hydrophobic	Pi-Alkyl
5		-130.203	0					ILE 235	2.54528	Hydrophobic	Pi-Sigma
								TRP 59	4.74934	Hydrophobic	Pi-Pi Stacked
								TRP 59	4.80932	Hydrophobic	Pi-Pi Stacked

							TYR 62	3.98784	Hydrophobic	Pi-Pi Stacked
							HIS 201	4.81125	Hydrophobic	Pi-Pi T-shaped
							HIS 201	4.40721	Hydrophobic	Pi-Pi T-shaped
							LEU 162	5.03737	Hydrophobic	Pi-Alkyl
							ALA 198	4.42415	Hydrophobic	Pi-Alkyl
							ALA 198	5.40498	Hydrophobic	Pi-Alkyl
							LYS 200	4.31606	Hydrophobic	Pi-Alkyl
6		0	HIS 201	2.75162	H-Bond	C-H Bond	TYR 62	4.15215	Hydrophobic	Pi-Pi T-shaped
							HIS 201	4.43183	Hydrophobic	Pi-Pi T-shaped
	-119.764						ALA 198	4.84588	Hydrophobic	Pi-Alkyl
							LYS 200	4.34686	Hydrophobic	Pi-Alkyl
							ILE 135	4.58754	Hydrophobic	Pi-Alkyl
7		0	HIS 201	2.46059	H-Bond	C-H Bond	TRP 59	4.84033	Hydrophobic	Pi-Pi Stacked
							TYR 62	4.11739	Hydrophobic	Pi-Pi Stacked
							HIS 201	4.49527	Hydrophobic	Pi-Pi T-shaped
	-128.486						ALA 198	4.96571	Hydrophobic	Pi-Alkyl
							LYS 200	4.35017	Hydrophobic	Pi-Alkyl
							ILE 135	4.4765	Hydrophobic	Pi-Alkyl
Acarbose		-	ASP 197	1.8105	H-Bond	Conventional	LEU 165	4.88528	Hydrophobic	Alkyl
		14.100	ASP 300	1.95489	H-Bond	H-Bond				
		9	ASP 197	1.62316	H-Bond	Conventional				
			HIS 201	1.89935	H-Bond	H-Bond				
			GLU 233	2.26313	H-Bond	Conventional				
			HIS 305	2.04716	H-Bond	H-Bond				
			HIS 201	2.49215	H-Bond	Conventional				
	-111.221		TRP 59	2.648	H-Bond	H-Bond				
			ASP 300	2.67656	H-Bond	Conventional				
			GLU 233	2.82655	H-Bond	H-Bond				
			HIS 201	2.29714	H-Bond	Conventional				
			ASP 197	2.90335	H-Bond	H-Bond				
			ASP 356	3.05439	H-Bond	C-H Bond				
			HIS 305	2.86783	H-Bond	C-H Bond				

				TRP 59	2.60264	H-Bond	C-H Bond C-H Bond C-H Bond C-H Bond C-H Bond C-H Bond Pi-Donor C-H Bond				
1	**5U3A**	-129.595	-0.85637 5	GLN 63 THR 163	2.59631 2.63444	H-Bond H-Bond	Conventional H-Bond Pi-Donor C-H Bond	TRP 58 TYR 62 LEU 162 LEU 165 TRP 59 TYR 62 TYR 62 HIS 101 HIS 299 LEU 165 LEU 162	2.82436 4.13933 5.21172 4.41345 4.73249 5.18159 4.04032 3.97068 4.61241 5.21083 5.49875	Hydrophobic Hydrophobic Hydrophobic Hydrophobic Hydrophobic Hydrophobic Hydrophobic Hydrophobic Hydrophobic Hydrophobic Hydrophobic	Pi-Sigma Pi-Pi Stacked Alkyl Alkyl Pi-Alkyl Pi-Alkyl Pi-Alkyl Pi-Alkyl Pi-Alkyl Pi-Alkyl Pi-Alkyl
2		-136.814	0	HIS 101 ASP 300 ASP 300	2.974 3.61554 4.02402	H-Bond H-Bond H-Bond	C-H Bond Pi-Donor C-H Bond Pi-Donor C-H Bond	ILE 235 TYR 62 HIS 201 ALA 307 ILE 235 PHE 256 LYS 200 ILE 235	2.46327 4.03258 4.35594 4.15963 4.97331 4.31257 4.90096 4.57476	Hydrophobic Hydrophobic Hydrophobic Hydrophobic Hydrophobic Hydrophobic Hydrophobic Hydrophobic	Pi-Sigma Pi-Pi Stacked Pi-Pi T-shaped Alkyl Alkyl Pi-Alkyl Pi-Alkyl Pi-Alkyl
3		-132.725	-2.17434	GLN 63 ASP 300 ASP 300	2.18734 2.63534 2.90367	H-Bond H-Bond H-Bond	Conventional H-Bond C-H Bond C-H Bond	TYR 62 TRP 59 ILE 165	4.16282 5.26822 4.58755	Hydrophobic Hydrophobic Hydrophobic	Pi-Pi Stacked Pi-Pi T-shaped Pi-Alkyl

4		-5	LYS 200	3.00684	H-Bond	Conventional	HIS 201	4.2464	Hydrophobic	Pi-Pi T-shaped
			LYS 200	2.36806	H-Bond	H-Bond	ALA 307	3.80255	Hydrophobic	Alkyl
			LYS 200	2.12809	H-Bond	Conventional	ILE 235	4.76093	Hydrophobic	Alkyl
						H-Bond	PHE 256	4.29699	Hydrophobic	Pi-Alkyl
						Conventional	ILE 235	4.39493	Hydrophobic	Pi-Alkyl
						H-Bond	ALA 307	4.31011	Hydrophobic	Pi-Alkyl
	-132.011						LEU 162	5.32705	Hydrophobic	Pi-Alkyl
							ALA 198	4.95834	Hydrophobic	Pi-Alkyl
							LYS 200	5.39353	Hydrophobic	Pi-Alkyl
							ILE 235	4.78965	Hydrophobic	Pi-Alkyl
							I;E 235	4.60736	Hydrophobic	Pi-Alkyl
							ALA 307	5.40135	Hydrophobic	Pi-Alkyl
5			ASP 300	3.60252	H-Bond	Pi-Donor C-H Bond	TRP 58	4.98877	Hydrophobic	Pi-Pi Stacked
							HIS 201	4.36037	Hydrophobic	Pi-Pi T-shaped
							ARG 303	4.73246	Hydrophobic	Pi-Alkyl
							LEU 162	4.80283	Hydrophobic	Pi-Alkyl
	-153.67	-7.4467					ALA 198	4.8166	Hydrophobic	Pi-Alkyl
							ALA 198	4.69767	Hydrophobic	Pi-Alkyl
							LYS 200	4.98611	Hydrophobic	Pi-Alkyl
							ILE 235	4.59203	Hydrophobic	Pi-Alkyl
6			THR 163	2.8	H-Bond	Conventional	TRP 58	2.83849	Hydrophobic	Pi-Sigma
			THR 163	2.97866	H-Bond	H-Bond	TRP 59	5.85015	Hydrophobic	Pi-Pi Stacked
	-119.52	-4.4269				C-H Bond	TRP 59	5.72454	Hydrophobic	Pi-Pi Stacked
							ARG 303	4.80812	Hydrophobic	Pi-Alkyl
							LEU 165	5.06341	Hydrophobic	Pi-Alkyl
7			GLN 63	2.87023	H-Bond	Conventional	TRP 58	3.02622	Hydrophobic	Pi-Sigma
			THR 163	2.2062	H-Bond	H-Bond	ARAG 303	4.66403	Hydrophobic	Pi-Alkyl
			THR 163	2.45618	H-Bond	Conventional				
	-137.62	0	THR 163	2.27296	H-Bond	H-Bond				
			THR 163	2.93759	H-Bond	Conventional				
			THR 163	2.35082	H-Bond	H-Bond				
						Conventional				

						H-Bond				
						C-H Bond				
						C-H Bond				
Acarbose		-21.557	LYS 200	2.8504	H-Bond	Conventional	LEU 165	3.2855	Hydrophobic	Alkyl
			LYS 200	2.42598	H-Bond	H-Bond	HIS 101	3.97636	Hydrophobic	Pi-Alkyl
			TRP 59	1.32563	H-Bond	Conventional				
			ASP 197	1.80631	H-Bond	H-Bond				
			ASP 300	1.83077	H-Bond	Conventional				
			THR 163	2.226	H-Bond	H-Bond				
			THR 163	2.20609	H-Bond	Conventional				
			ASP 197	1.66424	H-Bond	H-Bond				
			THR 163	1.75378	H-Bond	Conventional				
			THR 163	1.80251	H-Bond	H-Bond				
			TRP 59	2.91442	H-Bond	Conventional				
			ASP 197	2.94579	H-Bond	H-Bond				
			ASP 300	2.71705	H-Bond	Conventional				
	-118.885		GLU 233	2.93181	H-Bond	H-Bond				
			ASP 300	2.90226	H-Bond	Conventional				
			ASP 197	3.0589	H-Bond	H-Bond				
			HIS 201	2.24202	H-Bond	Conventional				
						H-Bond				
						Conventional				
						H-Bond				
						C-H Bond				
						C-H Bond				
						C-H Bond				
						C-H Bond				
						C-H Bond				
						C-H Bond				
						C-H Bond				

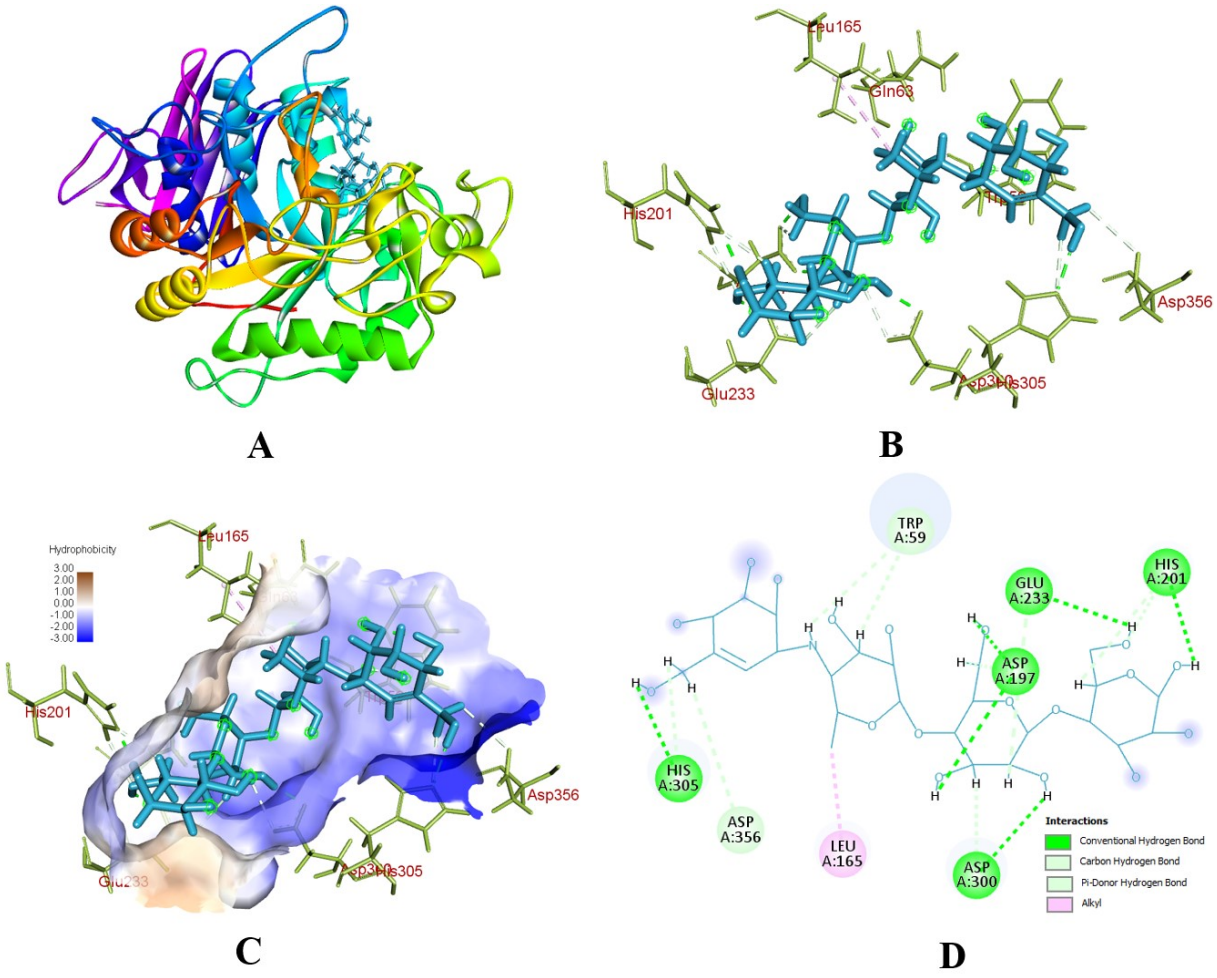

Figure S3: Interaction of 1SMD protein with Acarbose (A) structure of protein (B) protein-ligand interaction (C) hydrophobic interaction (D) 2D diagram of ligand

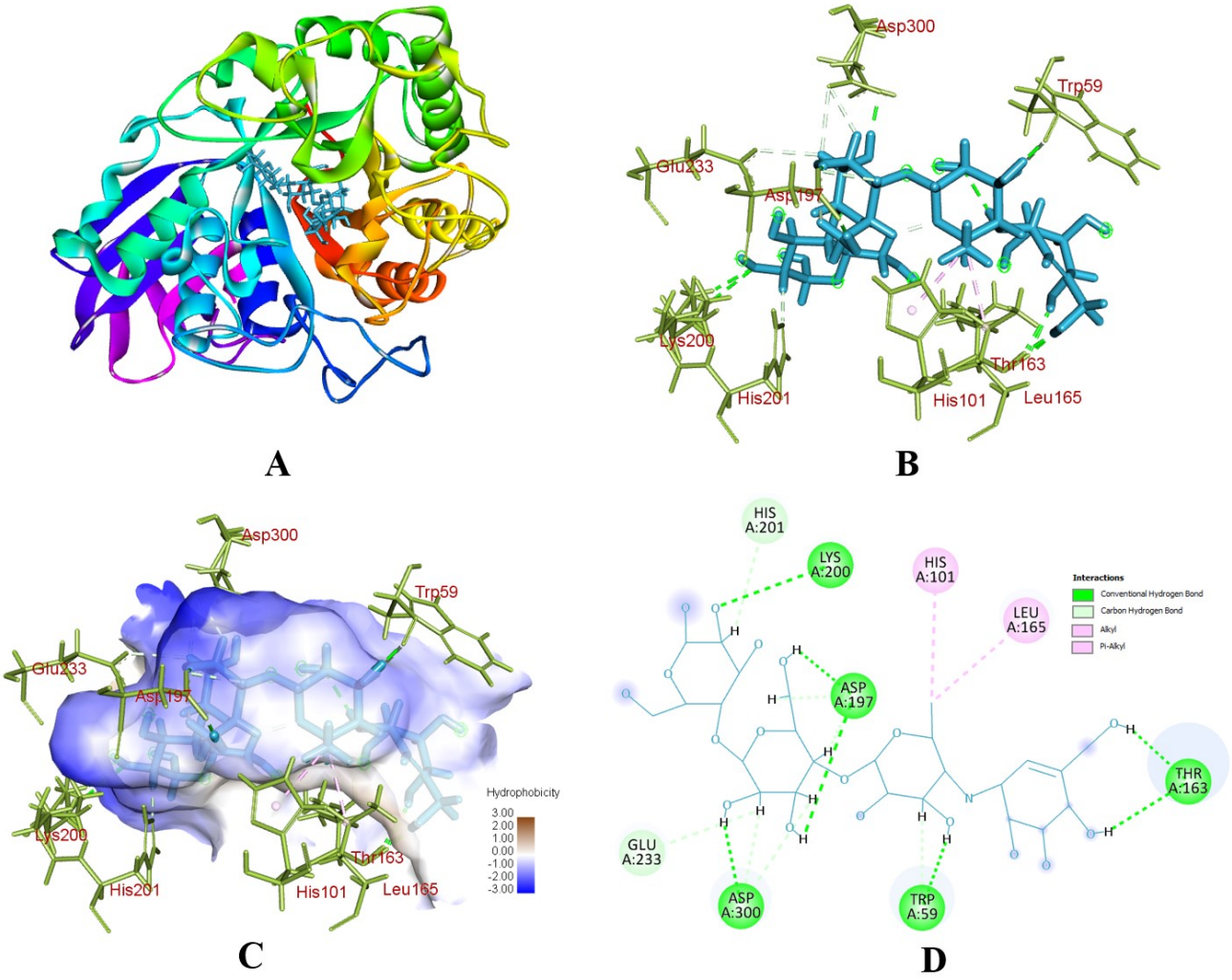

Figure S4: Interaction of 5U3A protein with Acarbose (A) structure of protein (B) protein-ligand interaction (C) hydrophobic interaction (D) 2D diagram of ligand

2.3. DFT Study

Table S5: HOMO, LUMO, energy gap and the global quantum reactivity's calculated at DFT/B3LYP/6-311G level

	Formula	**Acarbose**	**Thiourea**	**Compound 5**	**Compound 7**
Dipole moment (Debye)		9.201717	6.197388	6.712490	5.573720
Electronic energy (Hartree)		-2387.101829	-548.228339	-1662.361236	-1713.182469
LUMO (Hartree)		-0.01456	-0.00672	-0.13624	-0.14741
HOMO (Hartree)		-0.21573	-0.21029	-0.24412	-0.24634
Energy gap (Hartree)	$E_{HOMO} - E_{LUMO}$	0.20117	0.20357	0.10788	0.09893
Electron Affinity (A, Hartree)	$A = -E_{LUMO}$	0.01456	0.00672	0.13624	0.14741
Ionization Potential (I, Hartree)	$I = -E_{HOMo}$	0.21573	0.21029	0.24412	0.24634
Chemical potential (μ, Hartree)	$\mu = 1/2 (I + A)$	0.11515	0.10851	0.19018	0.19688
Electronegativity (χ, Hartree)	$\chi = -1/2 (I + A)$	-0.11515	-0.10851	-0.19018	-0.19688
Chemical hardness (η, Hartree)	$\eta = 1/2 (I - A)$	0.10059	0.10179	0.05394	0.04947
Chemical softness (S, $Hartree^{-1}$)	$S = 1/ \eta$	9.94	9.83	18.54	20.22
Electrophilicity index (ω, Hartree)	$\omega = 2(\mu^2/ \eta)$	0.0659	0.0578	0.3353	0.3918
Neucleophilicity index (N, $Hartree^{-1}$)	$N = 1/ \omega$	15.17	17.29	2.98	2.55
Additional electronic charge	$= - \mu / \eta$	-1.145	-1.066	-3.53	-3.98

FTIR Spectra of the Newly Synthesized Compounds

FTIR Spectrum of Compound 1

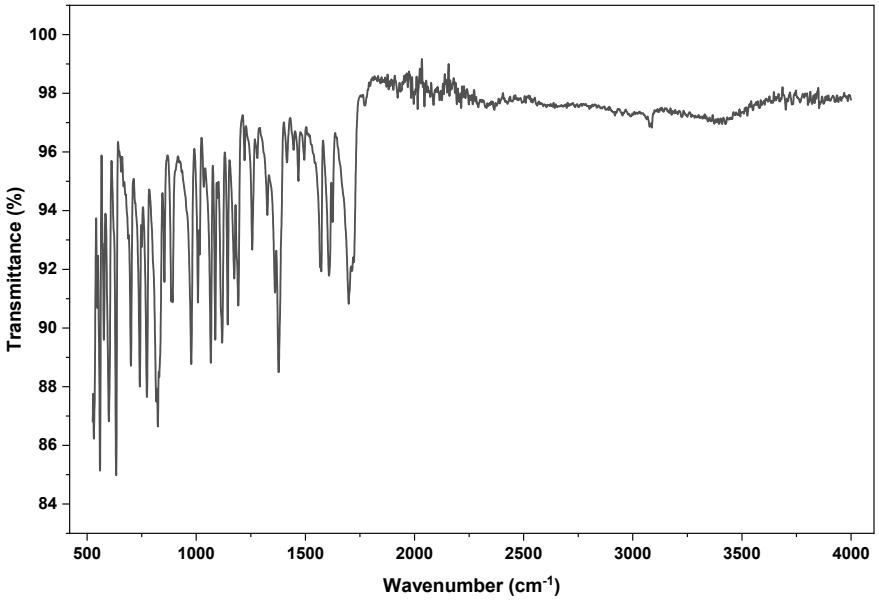

FTIR Spectrum of Compound 2

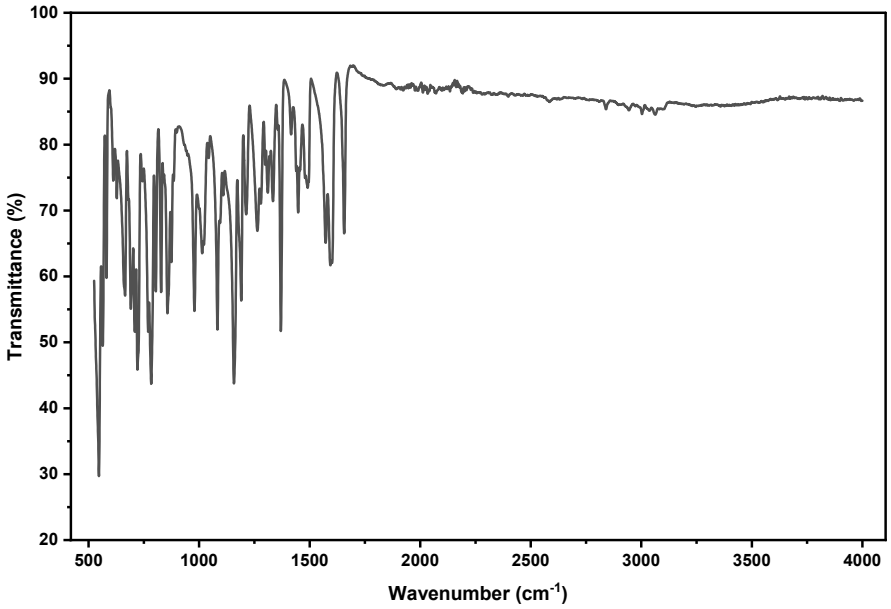

FTIR Spectrum of Compound 3

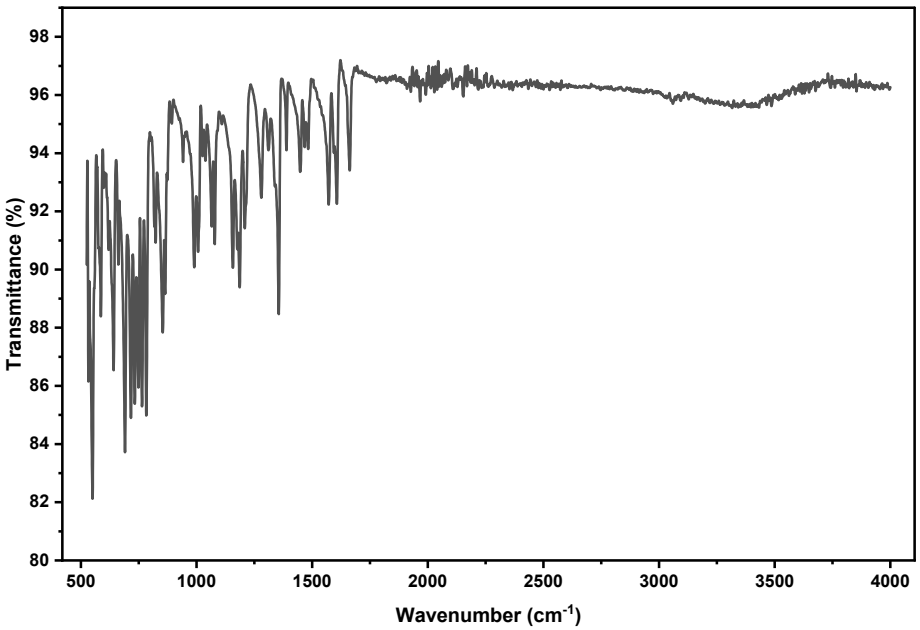

FTIR Spectrum of Compound 4

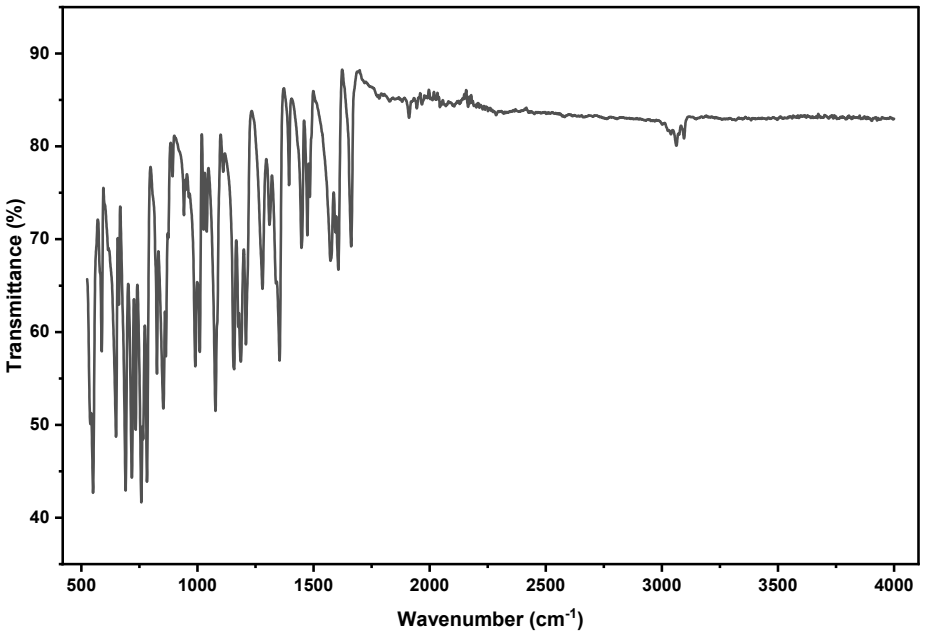

FTIR Spectrum of Compound 5

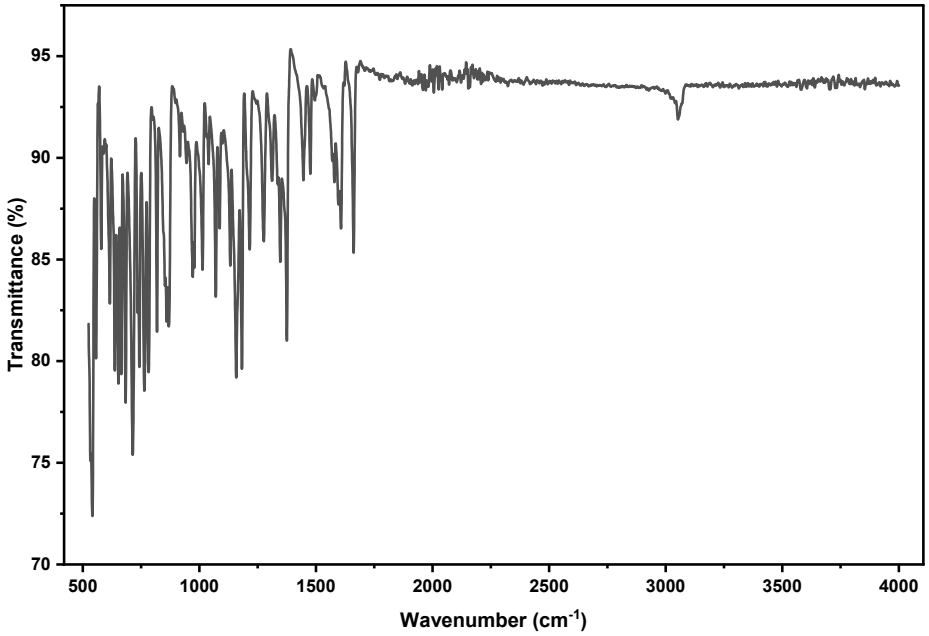

FTIR Spectrum of Compound 6

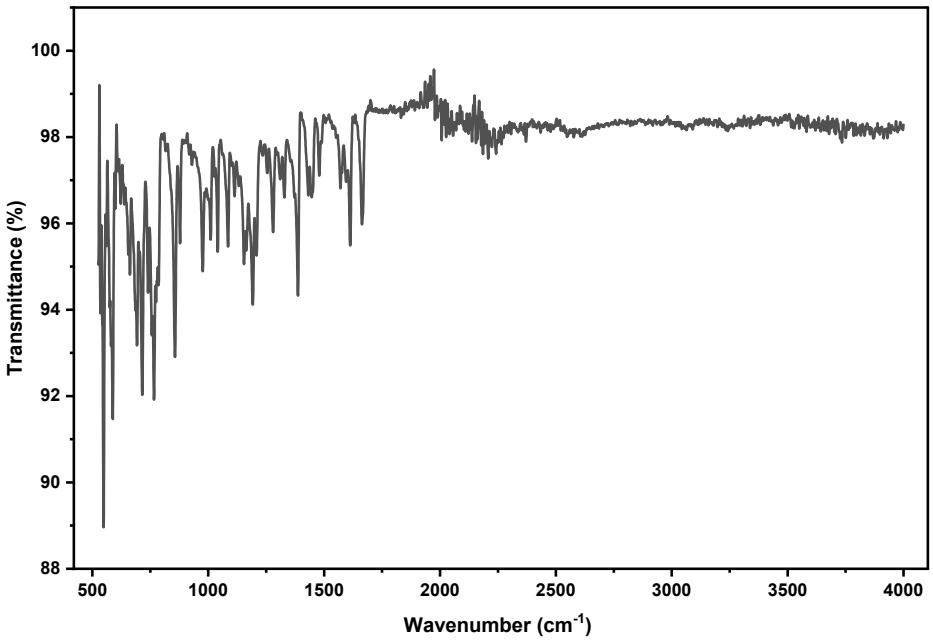

FTIR Spectrum of Compound 7

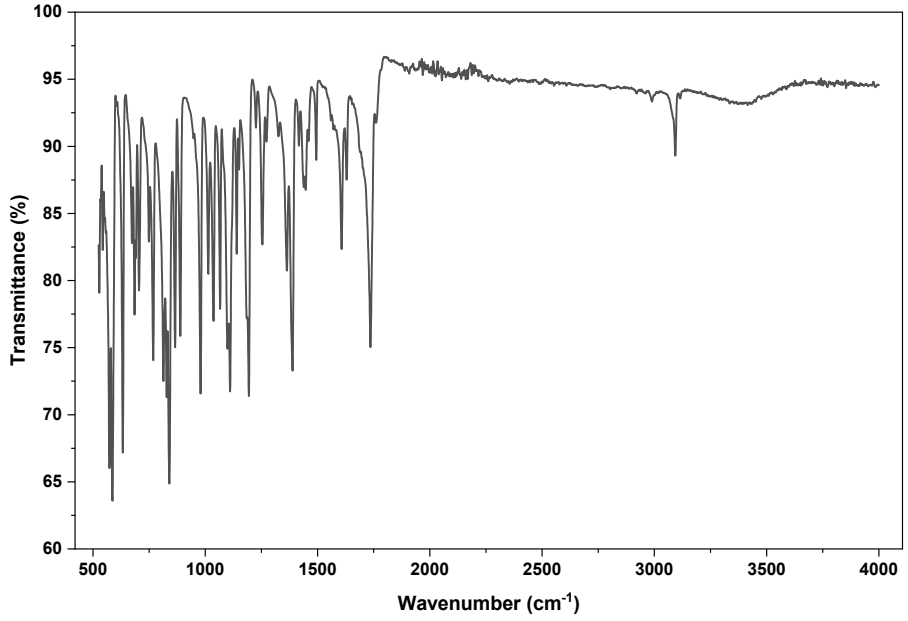

Mass Spectra of the Newly Synthesized Compounds

Mass Spectrum of Compound 1

FRUK I AHMED IAC-CH-01 #17-423 RT: 0.04-0.98 AV: 407 NL: 3.44E8
T: FTMS + p ESI Full ms [133.4000-1000.0000]

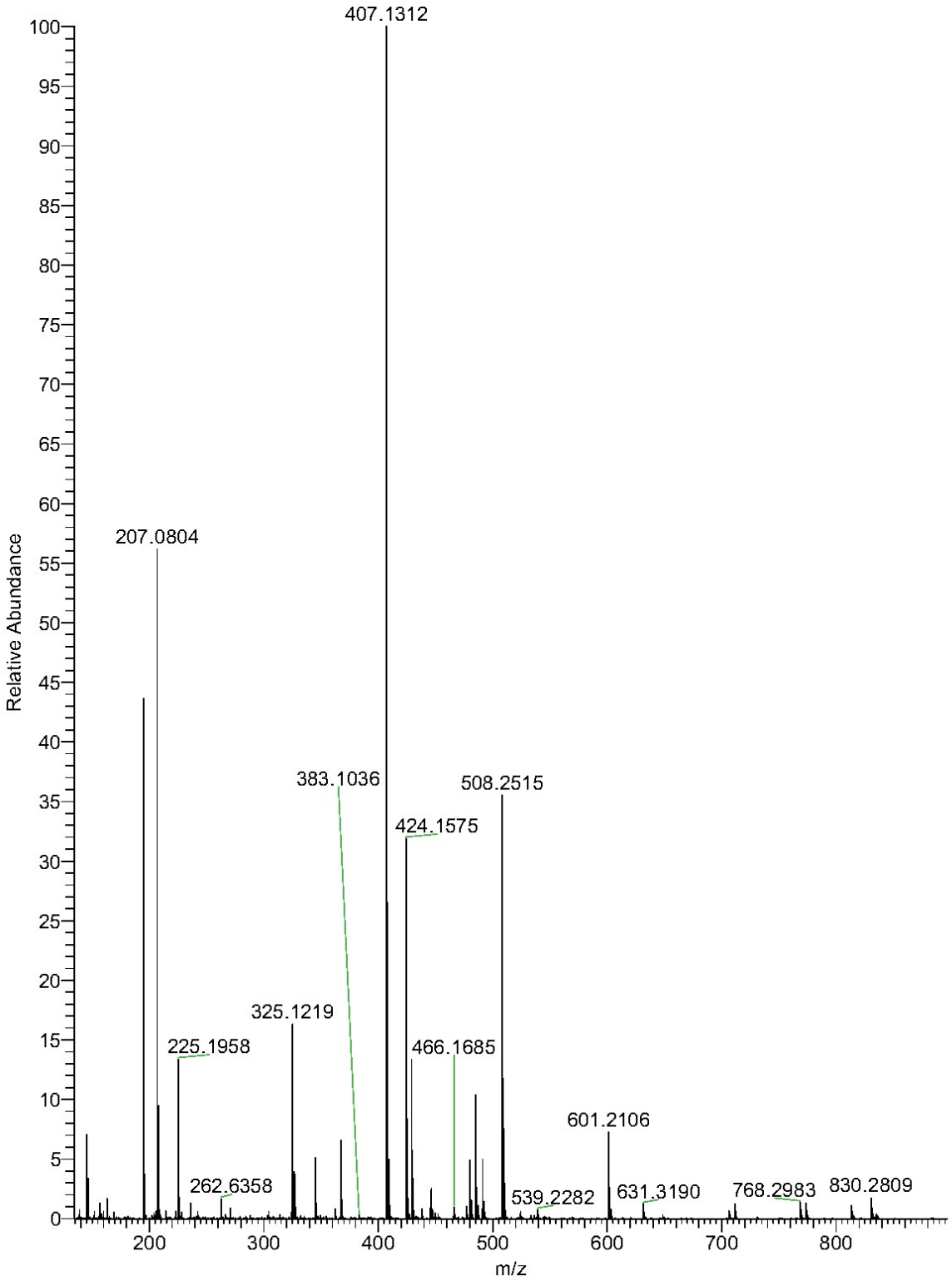

Mass Spectrum of Compound 2

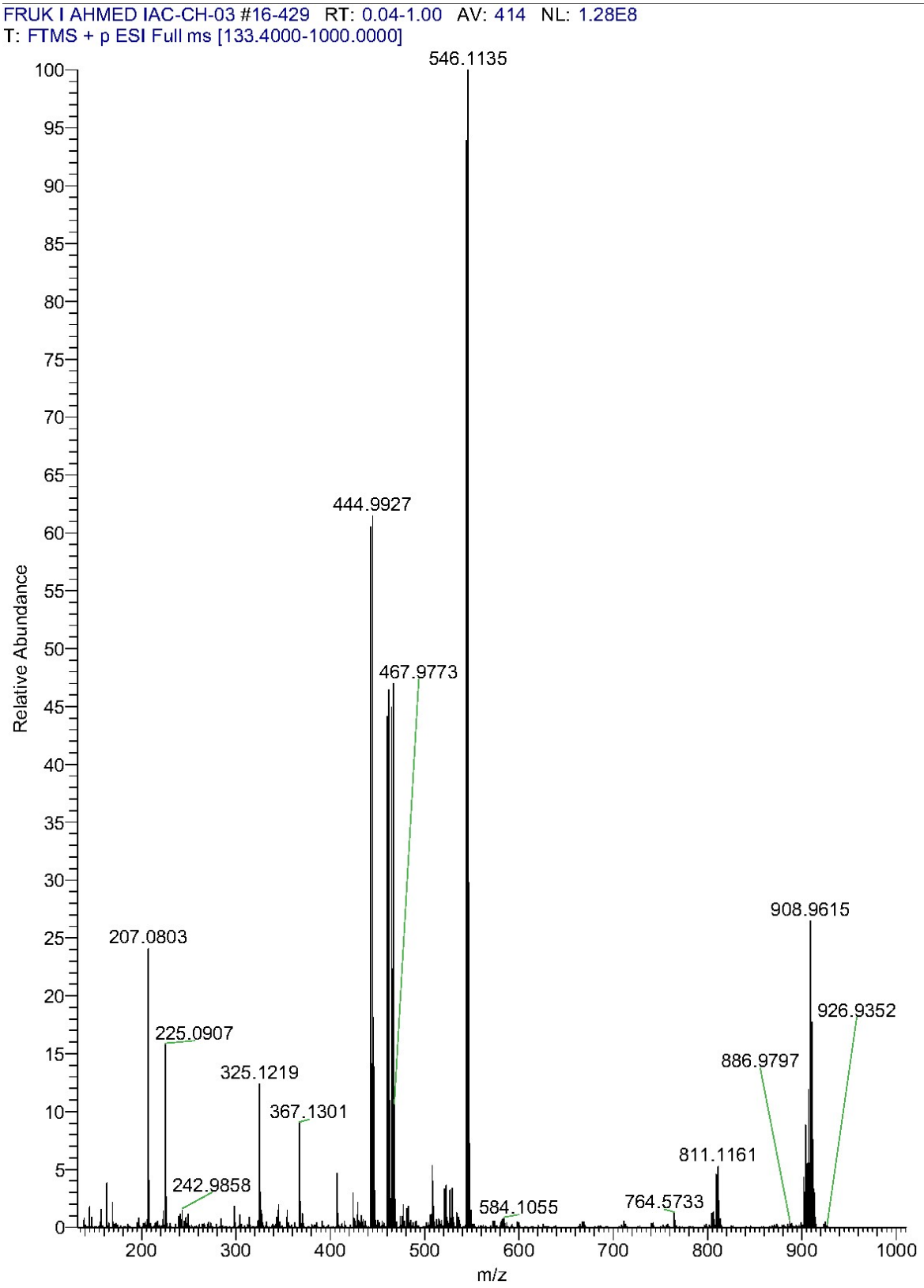

Mass Spectrum of Compound 3

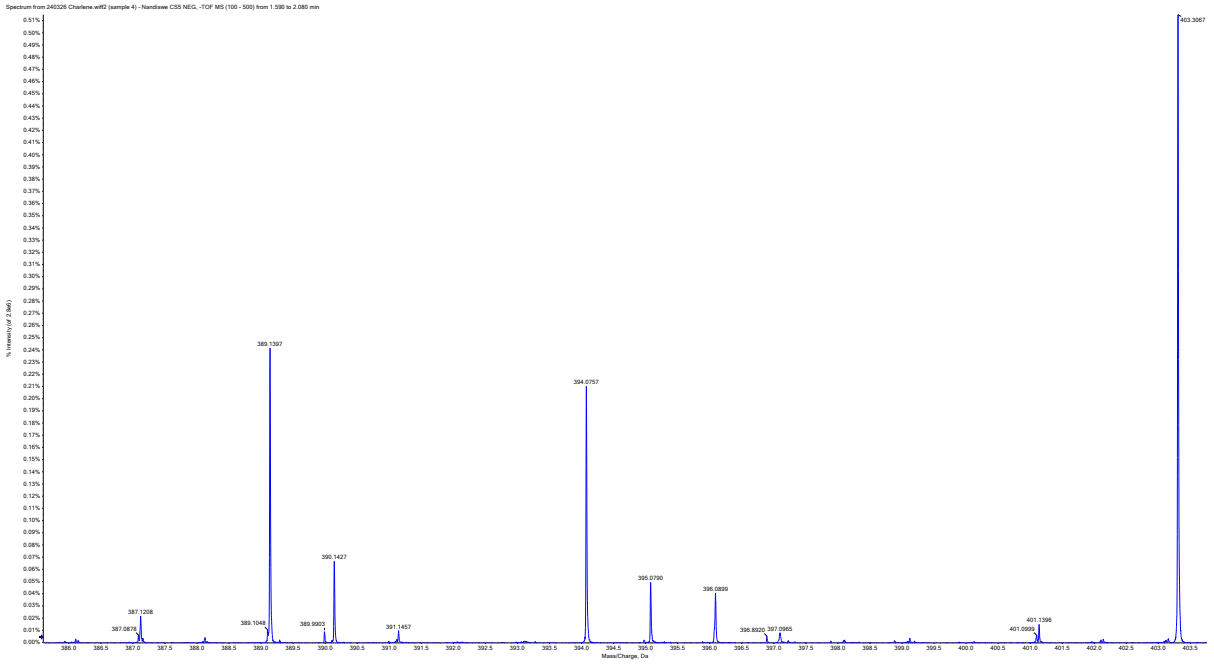

Mass Spectrum of Compound 4

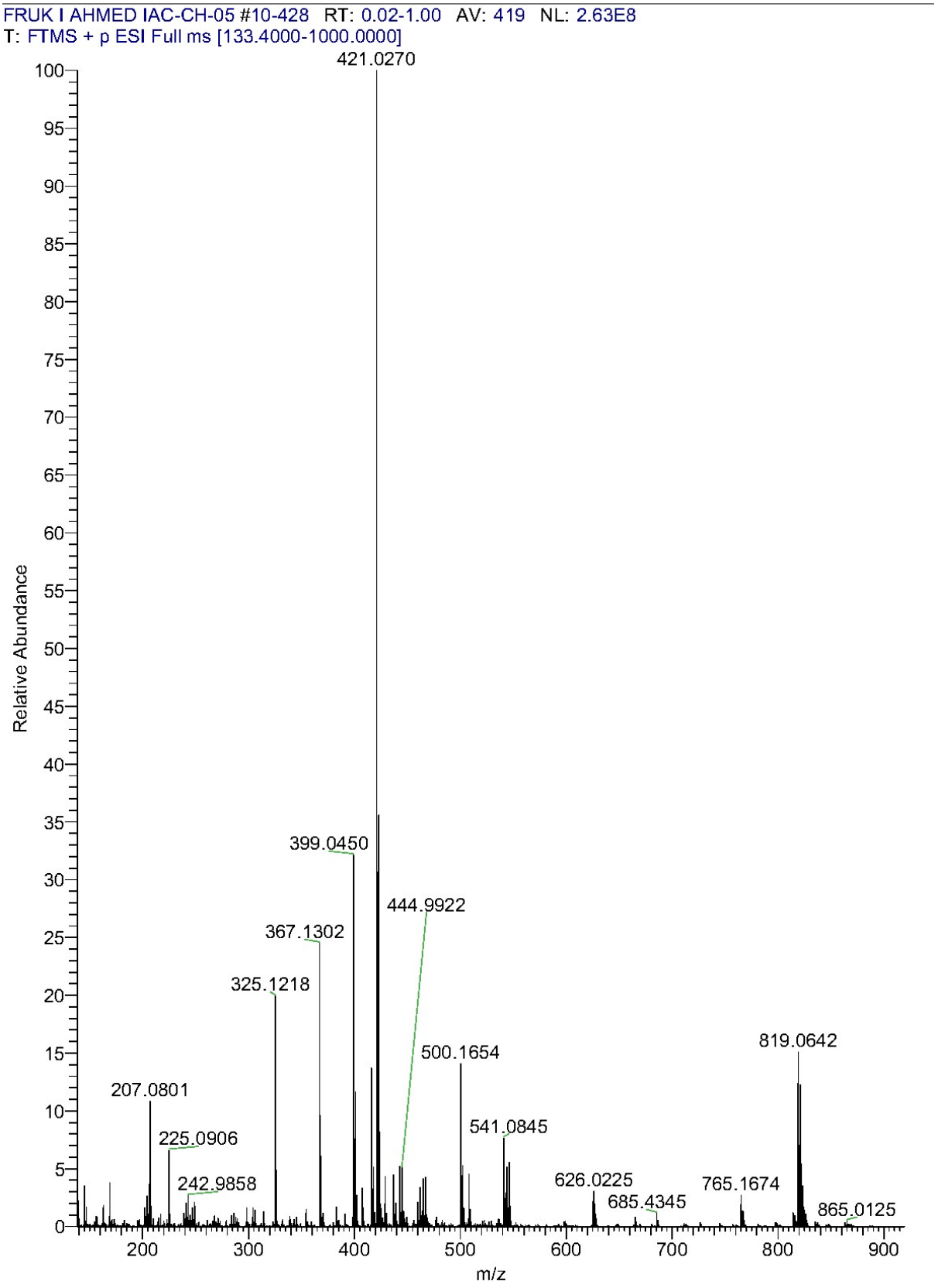

Mass Spectrum of Compound 5

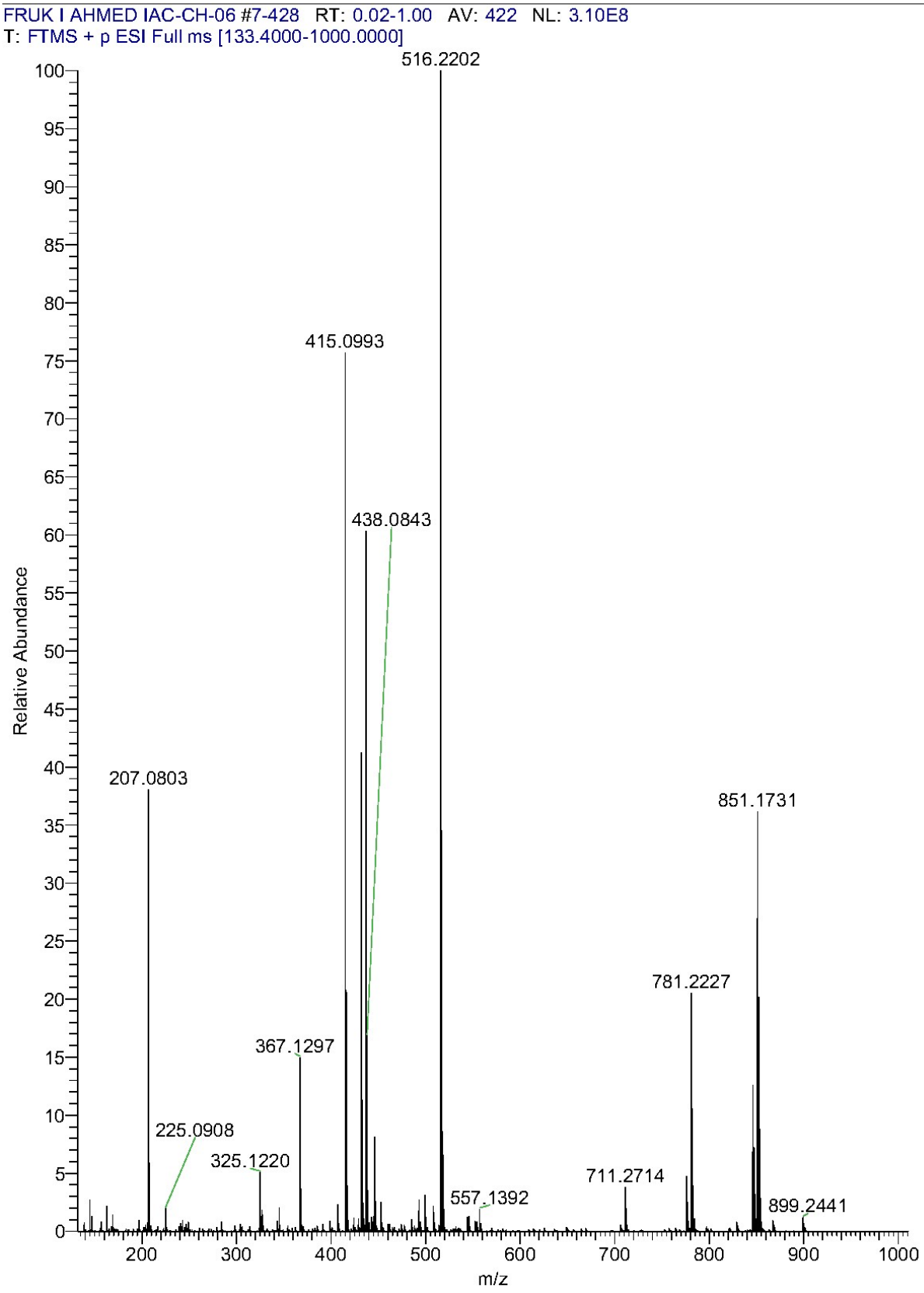

Mass Spectrum of Compound 6

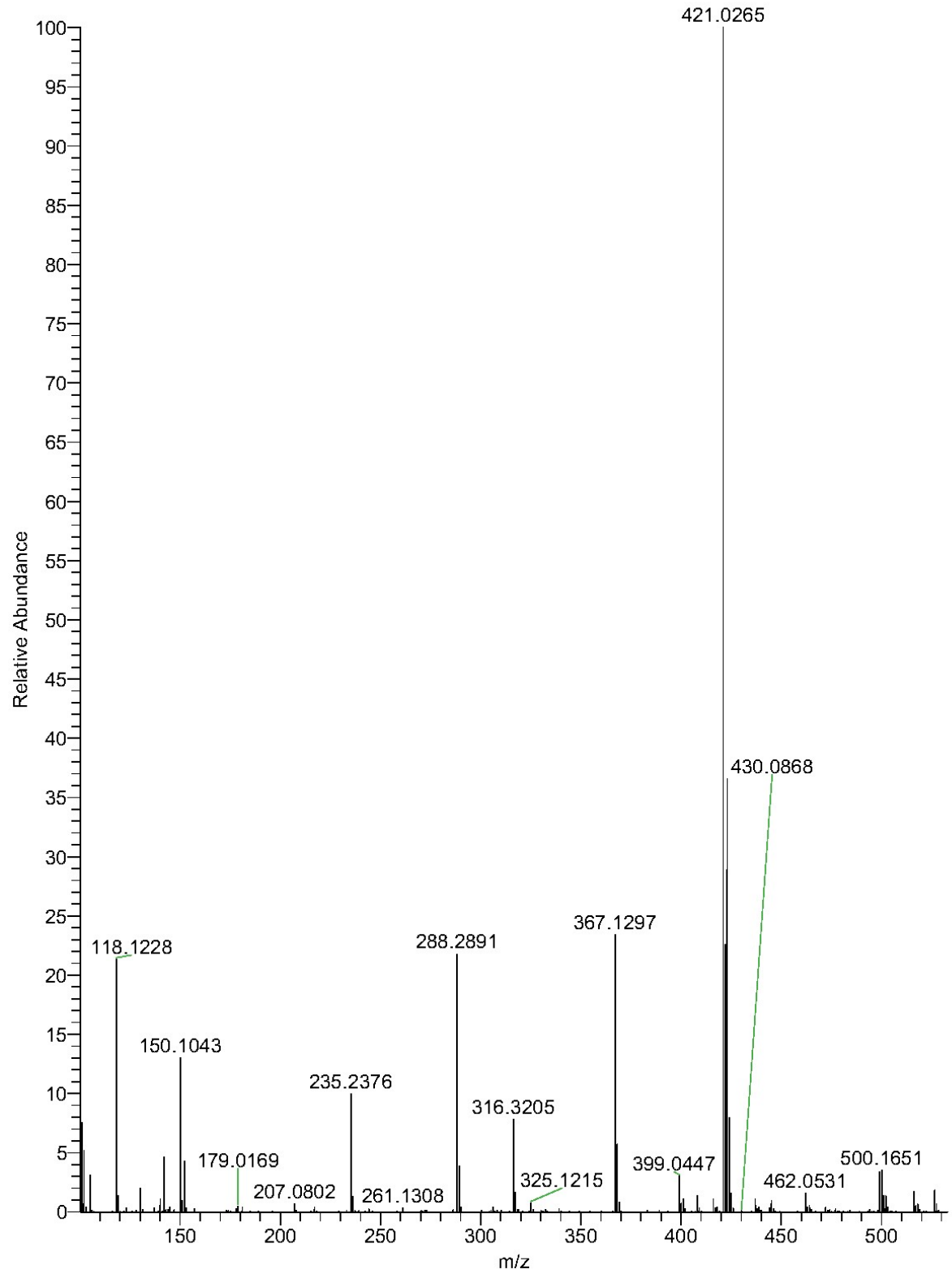

Mass Spectrum of Compound 7

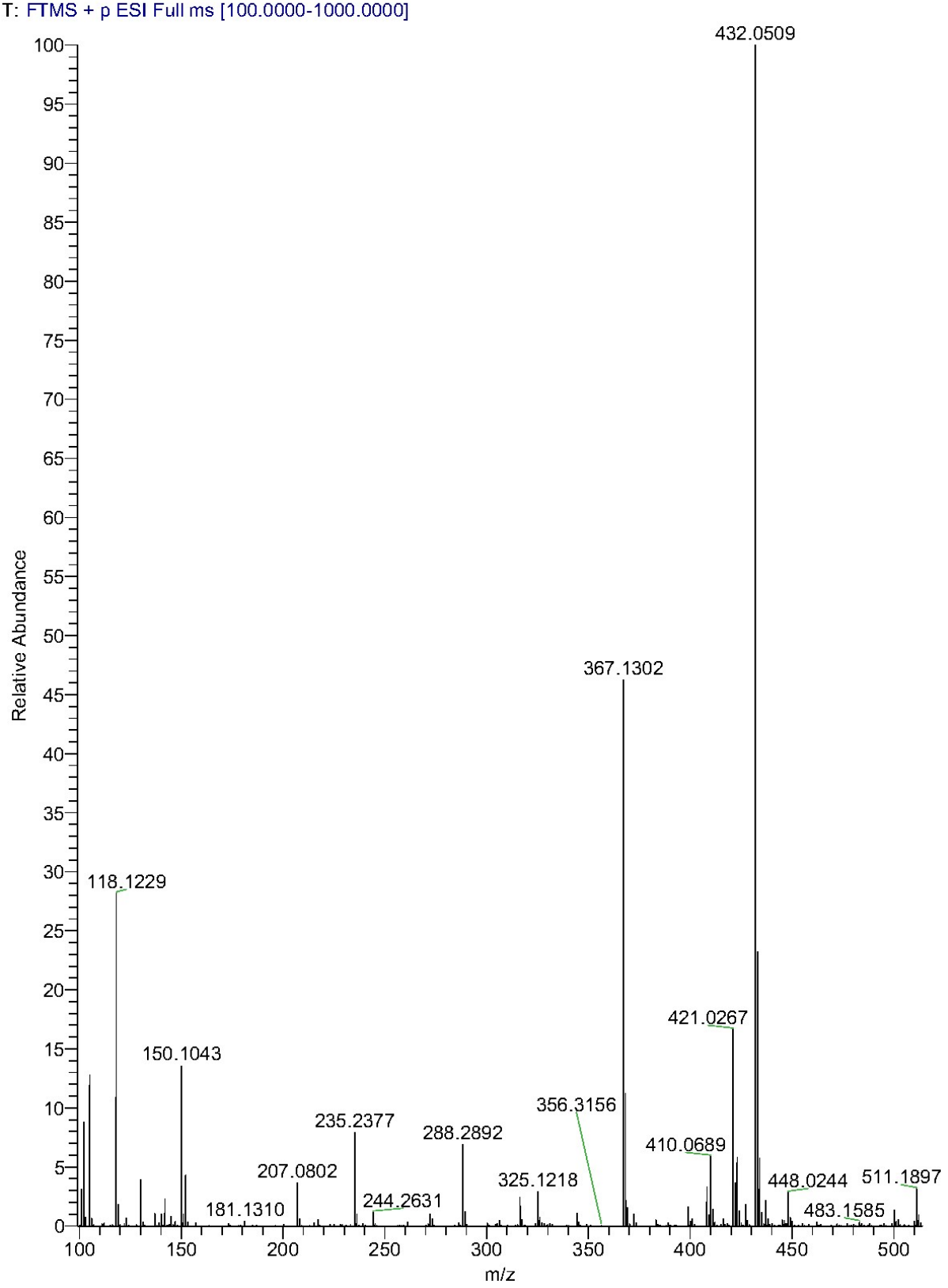

NMR Spectra of the Newly Synthesized Compounds

^{1}H-NMR Spectrum (400 MHz, $CDCl_3$) of Compound 1

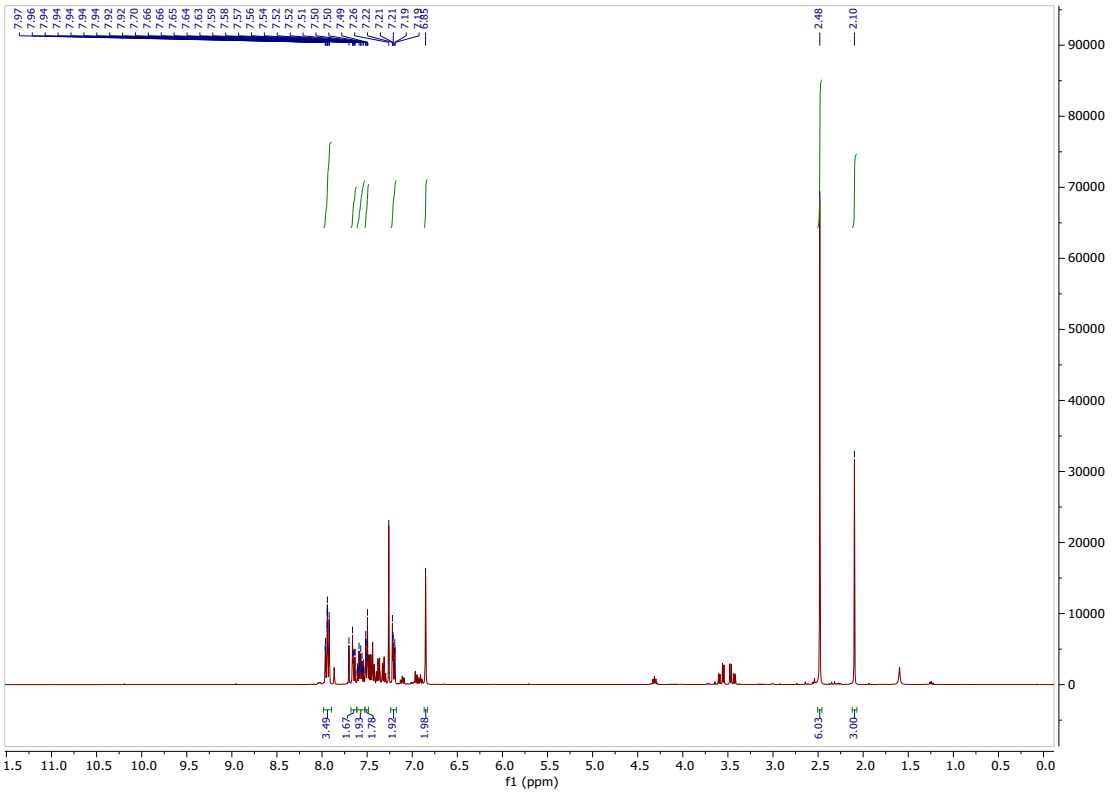

^{13}C-NMR Spectrum (101 MHz, $CDCl_3$) of Compound 1

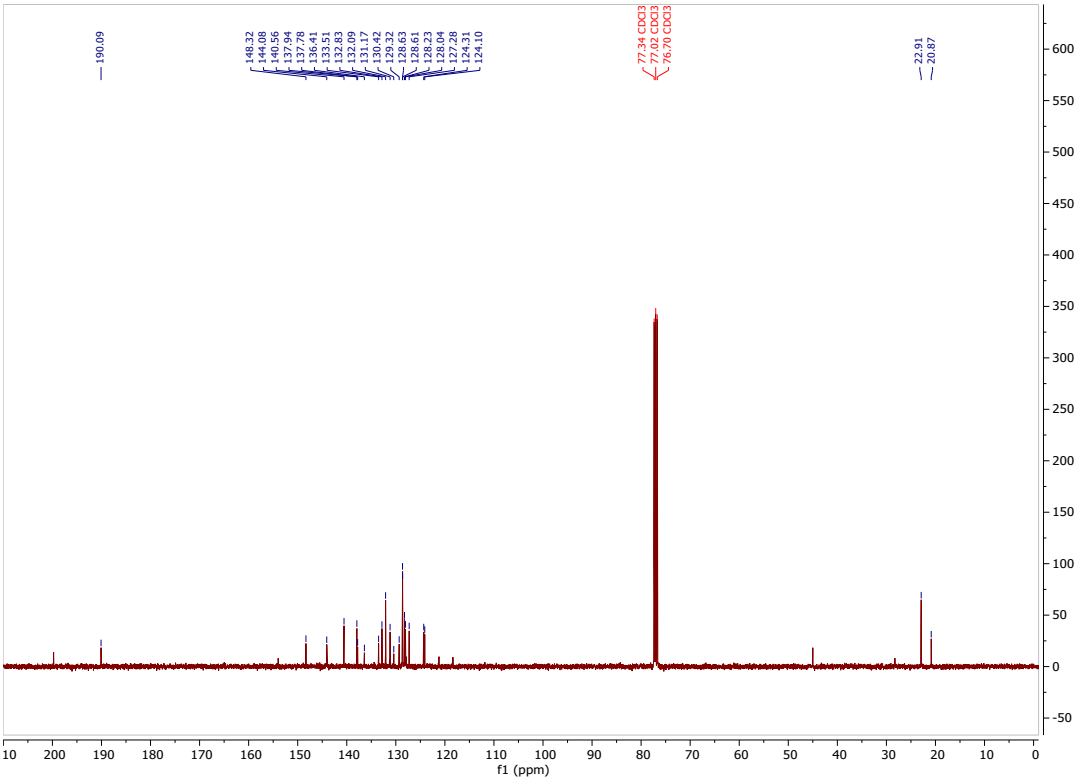

^{1}H-NMR Spectrum (400 MHz, $CDCl_3$) of Compound 2

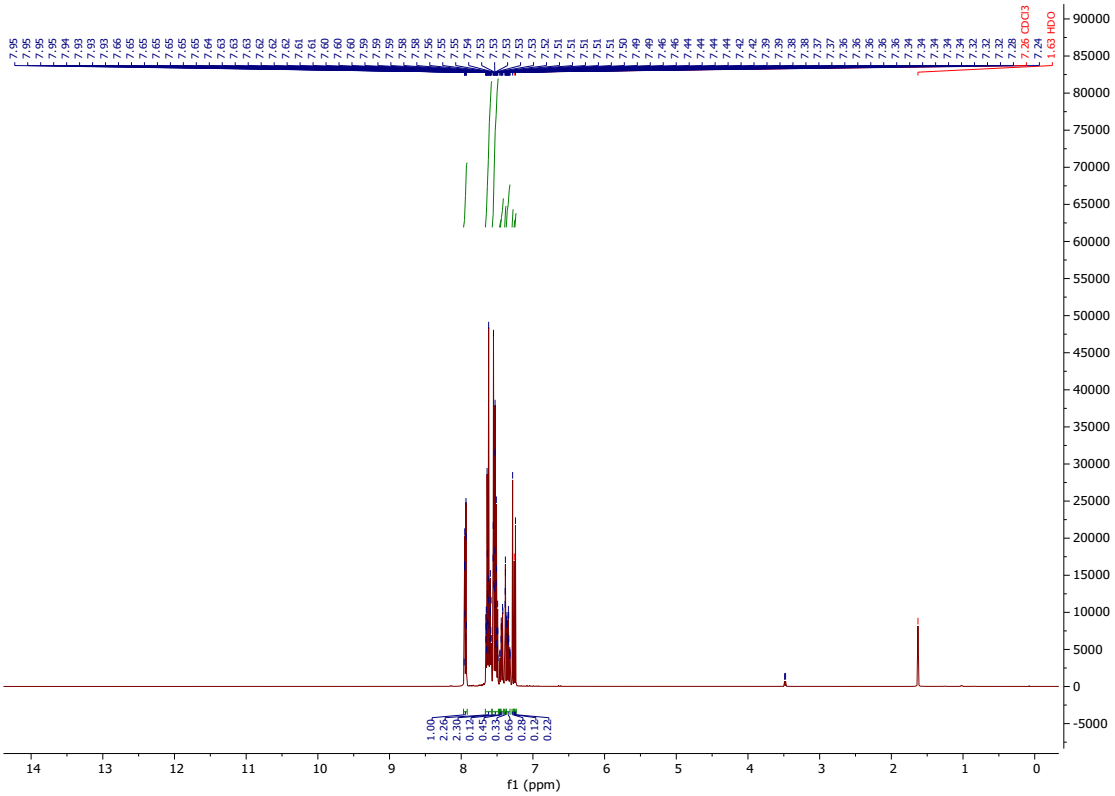

^{13}C-NMR Spectrum (101 MHz, $CDCl_3$) of Compound 2

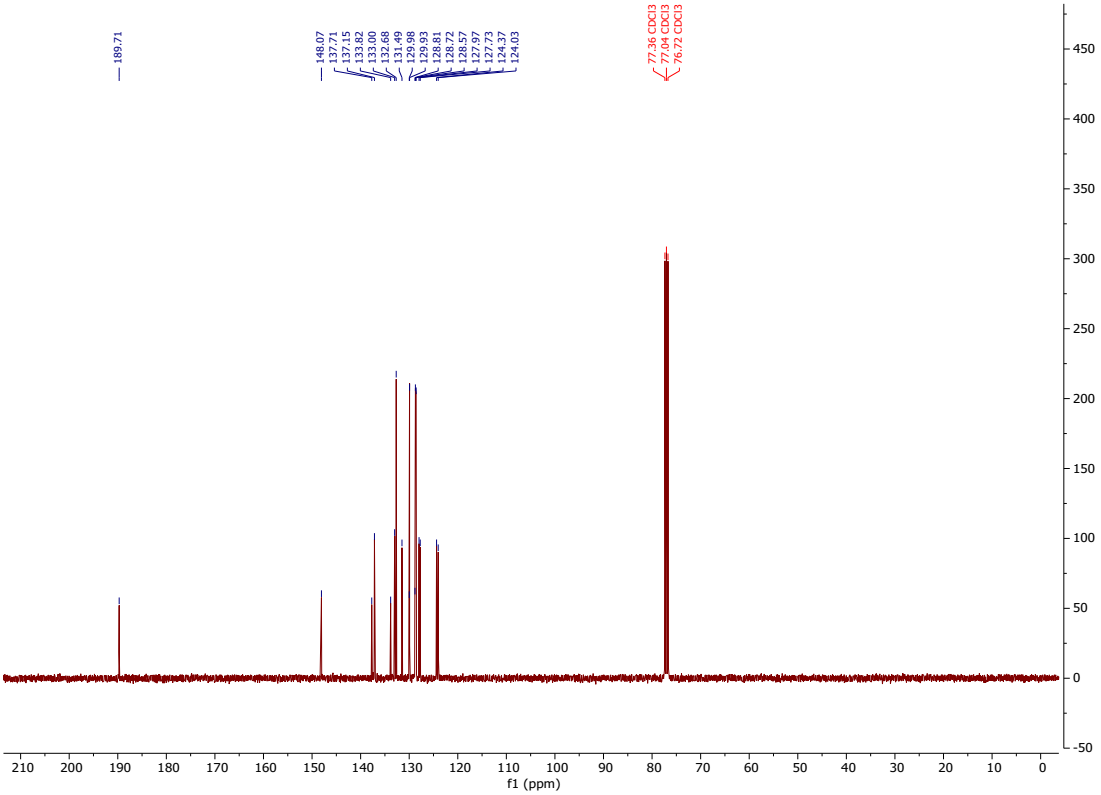

^{1}H-NMR Spectrum (600 MHz, $CDCl_3$) of Compound 3

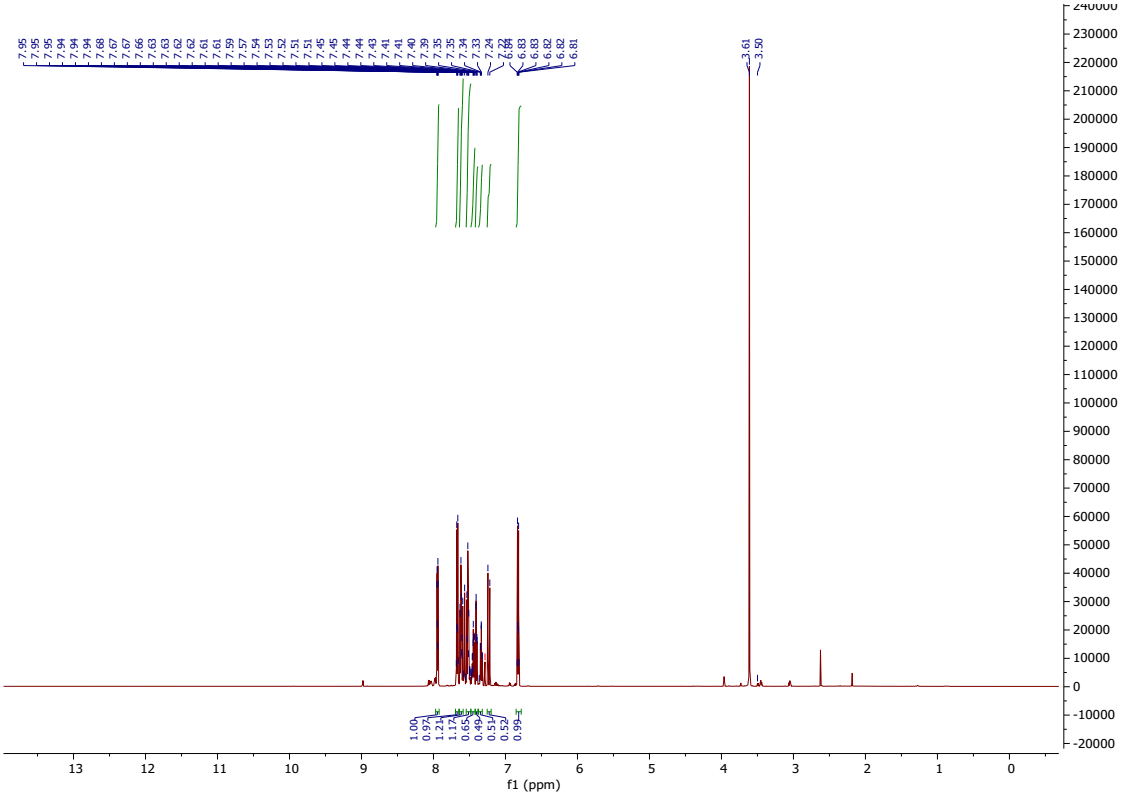

^{13}C-NMR Spectrum (151 MHz, $CDCl_3$) of Compound 3

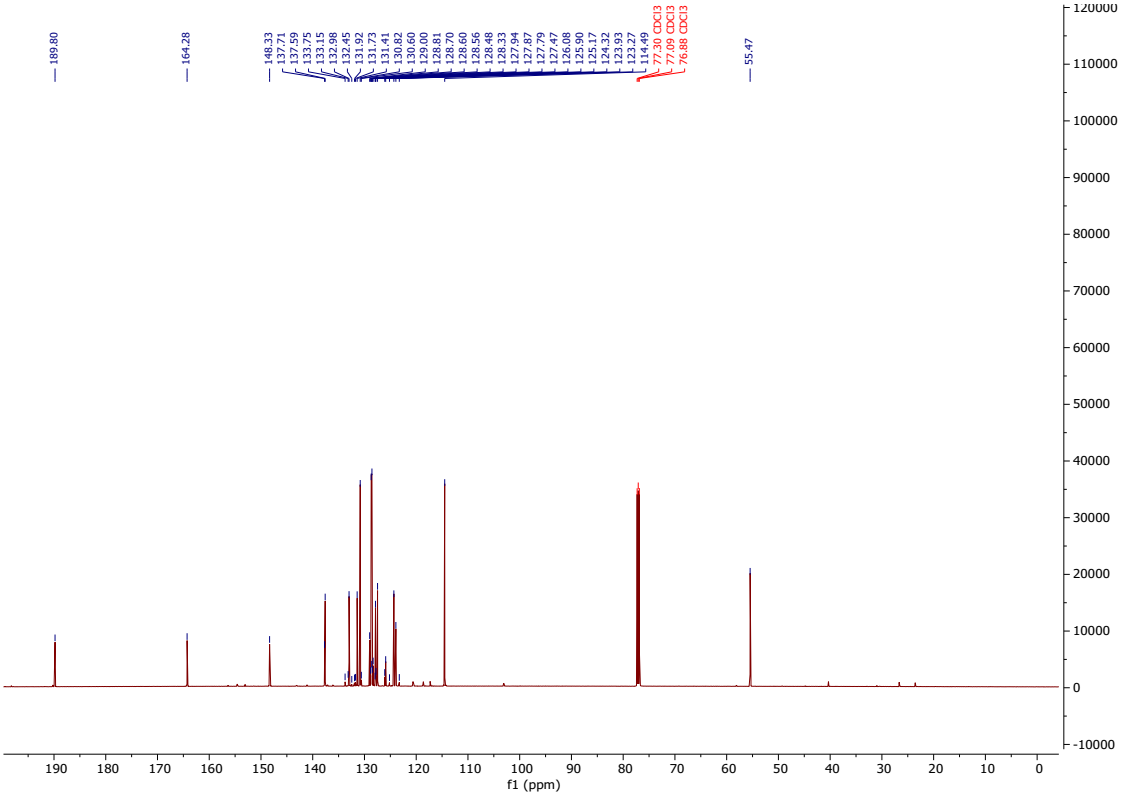

^{1}H-NMR Spectrum (400 MHz, $CDCl_3$) of Compound 4

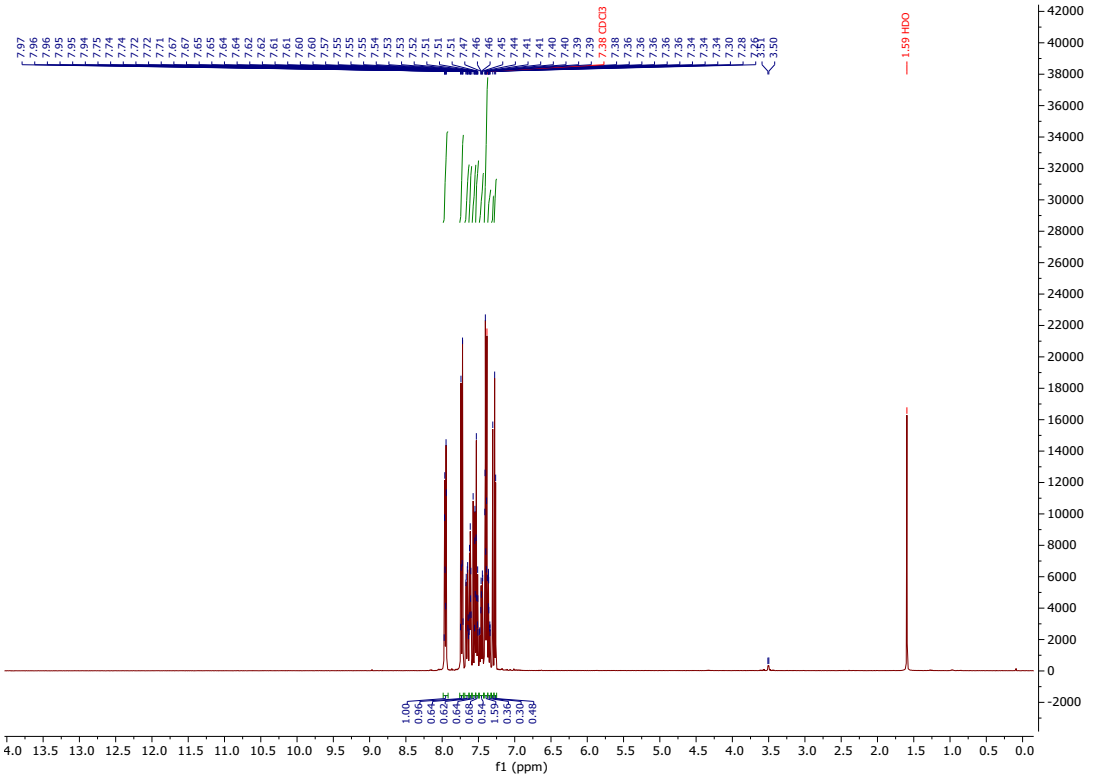

^{13}C-NMR Spectrum (101 MHz, $CDCl_3$) of Compound 4

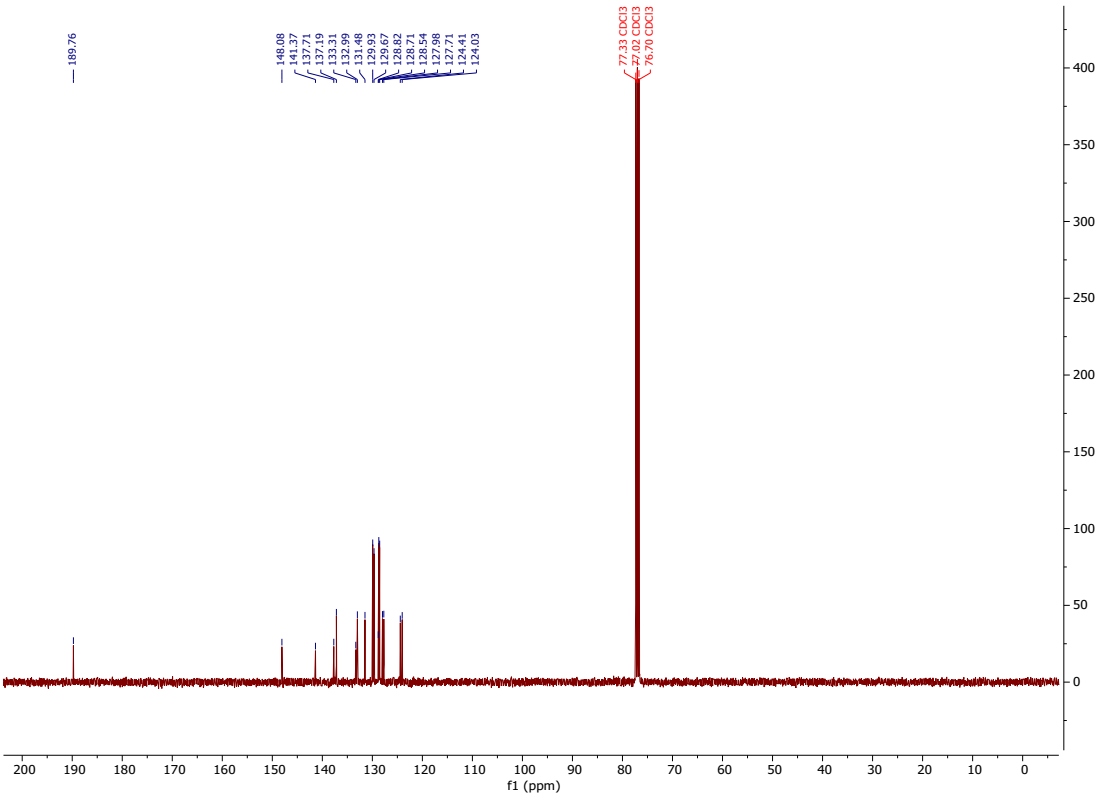

^{1}H-NMR Spectrum (400 MHz, $CDCl_3$) of Compound 5

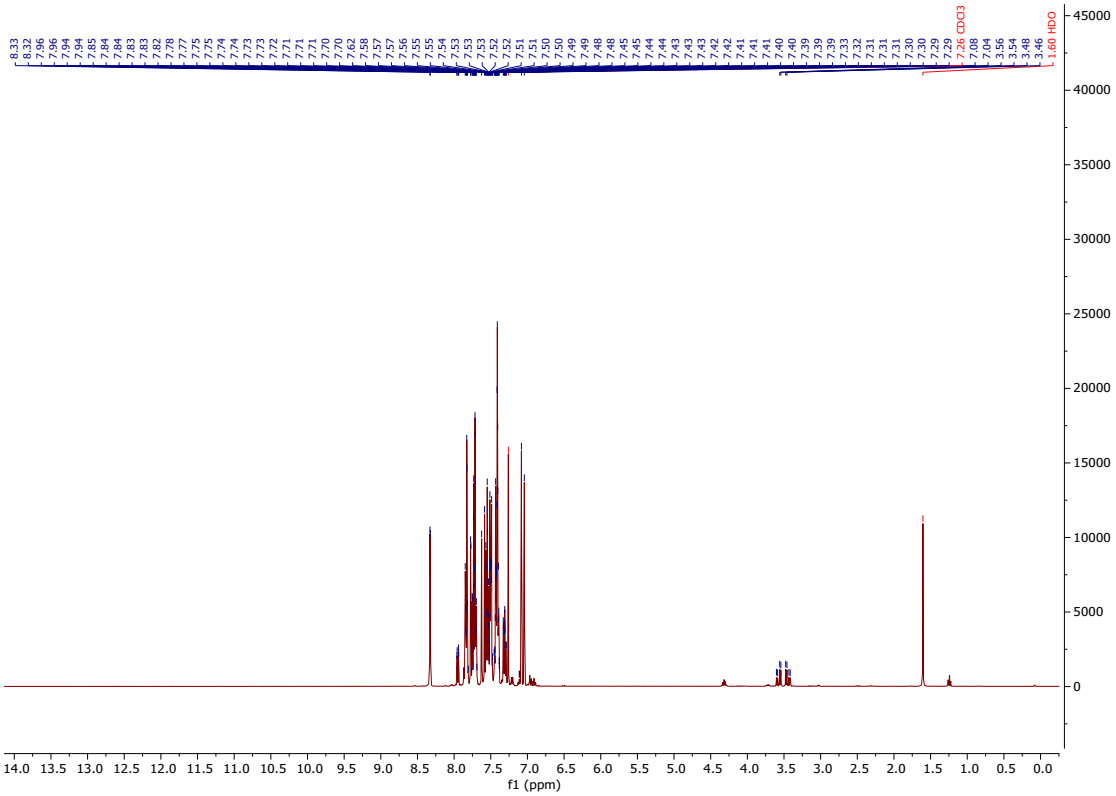

^{13}C-NMR Spectrum (101 MHz, $CDCl_3$) of Compound 5

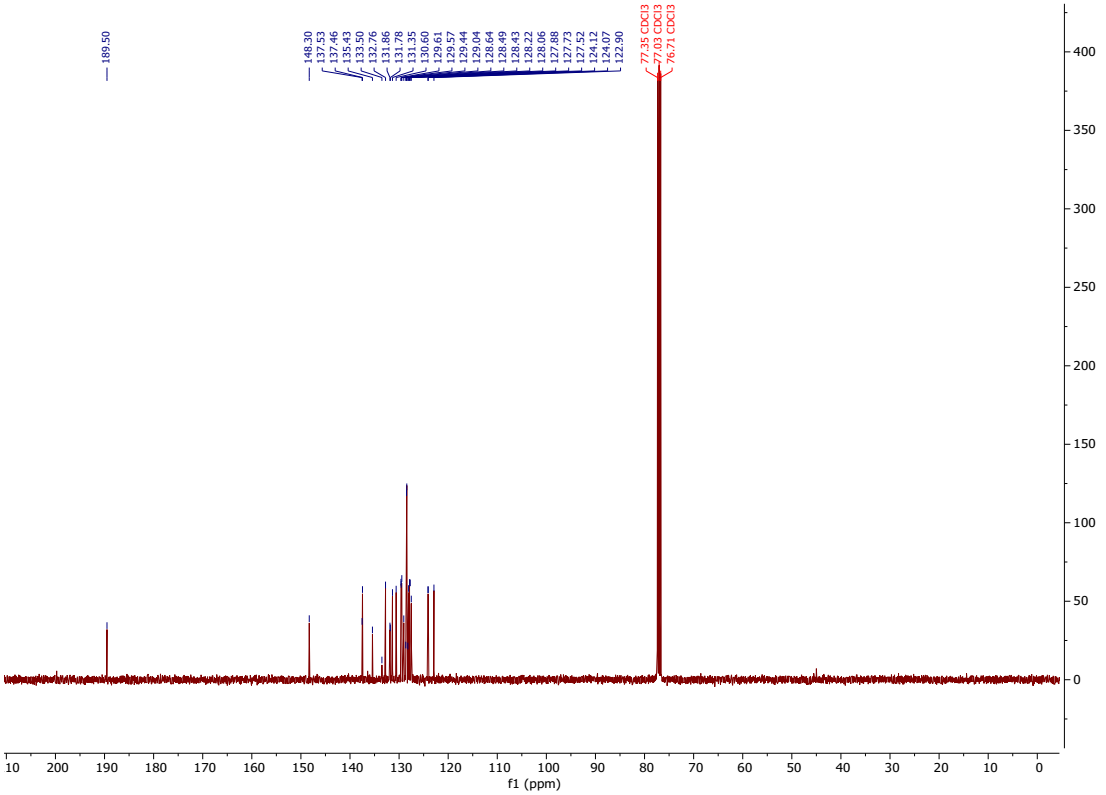

^{1}H-NMR Spectrum (400 MHz, $CDCl_3$) of Compound 6

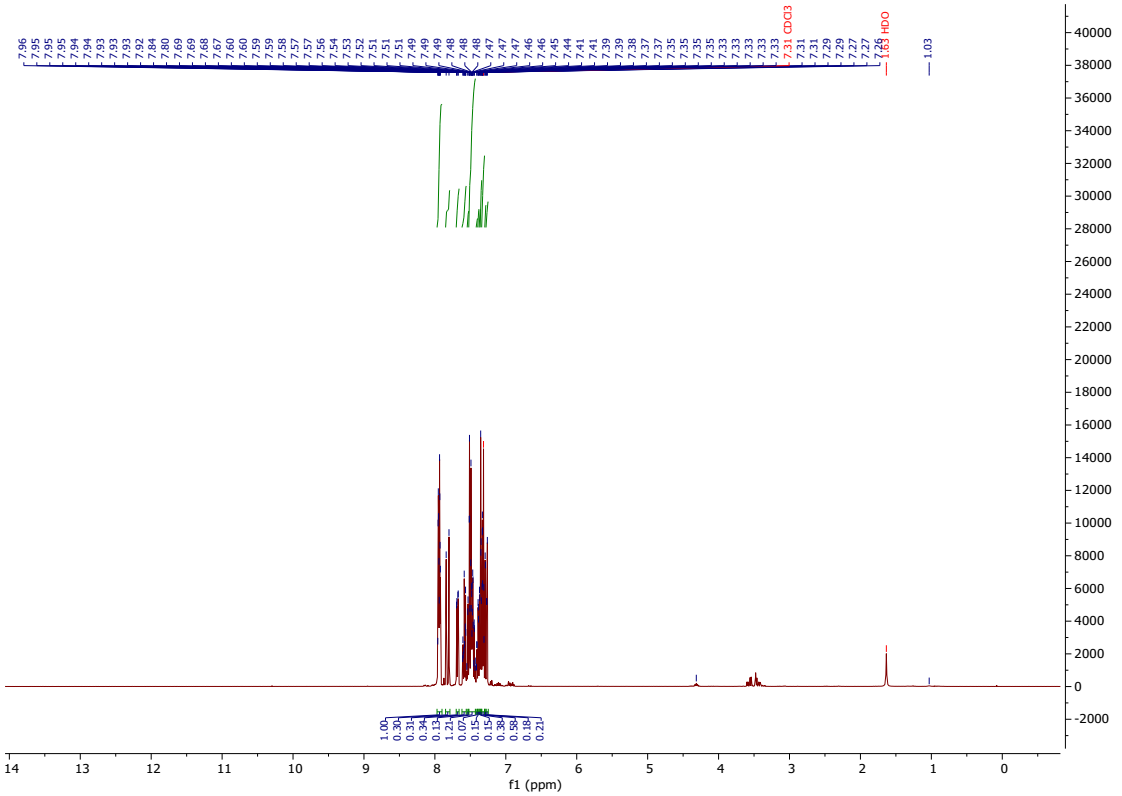

^{13}C-NMR Spectrum (101 MHz, $CDCl_3$) of Compound 6

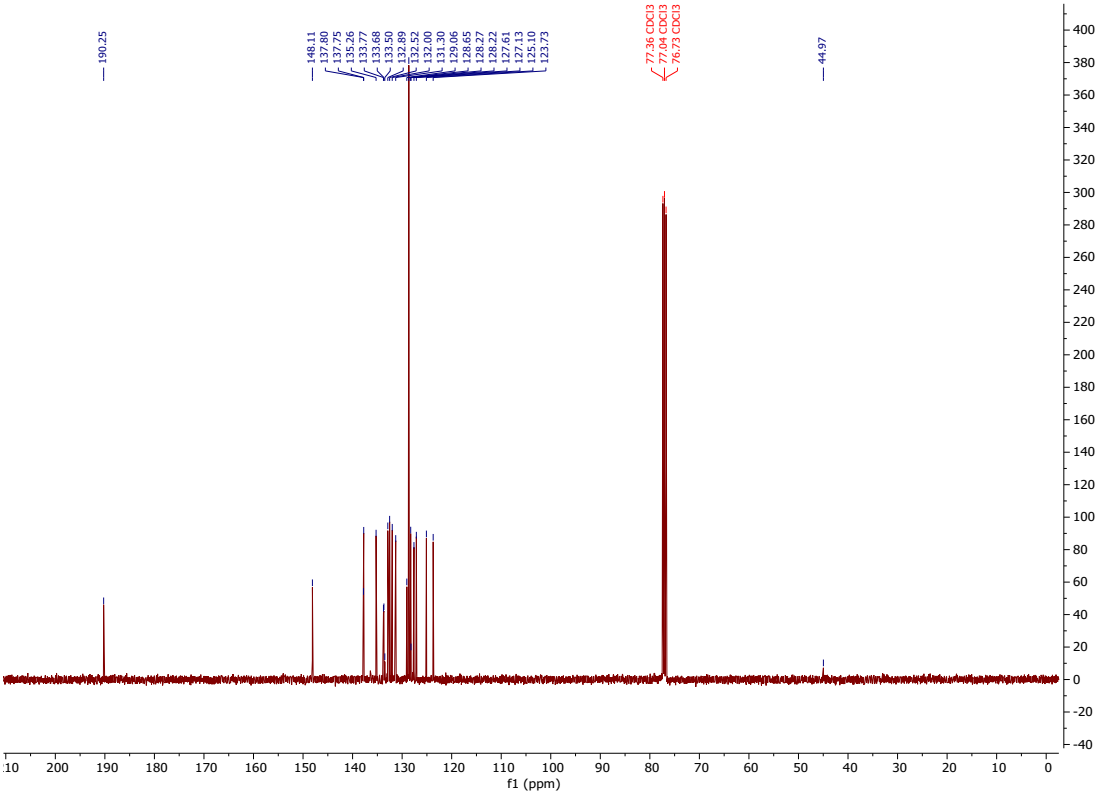

^{1}H-NMR Spectrum (400 MHz, $CDCl_3$) of Compound 7

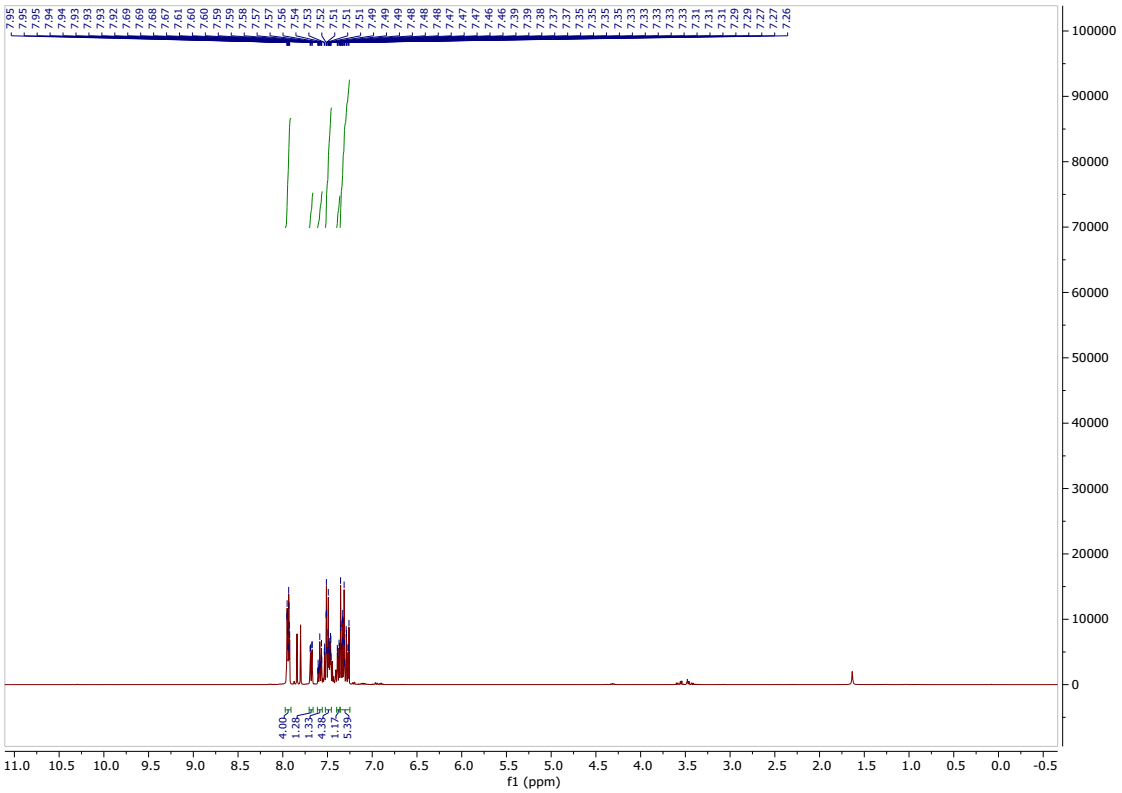

^{13}C-NMR Spectrum (101 MHz, $CDCl_3$) of Compound 7